

NASA Contractor Report NASA/CR-2002-211180

**Statistical Short-Range Guidance for Peak Wind Speed Forecasts
on Kennedy Space Center/Cape Canaveral Air Force Station:
Phase I Results**

Prepared by:
Winifred C. Lambert
Applied Meteorology Unit

Prepared for:
Kennedy Space Center
Under Contract NAS10-01052

NASA
National Aeronautics and
Space Administration

Office of Management

Scientific and Technical
Information Program
2002

THIS PAGE INTENTIONALLY BLANK

Executive Summary

The peak wind speeds are an important forecast element for both the Space Shuttle and Expendable Launch Vehicle (ELV) programs. As defined in the Shuttle Flight Rules (FR) and the Launch Commit Criteria (LCC), each vehicle is assigned certain peak wind thresholds that cannot be exceeded in order to ensure the safety of that vehicle during launch and/or landing operations. The 45th Weather Squadron (45 WS) and the Spaceflight Meteorology Group (SMG) indicate that peak winds are challenging to forecast, particularly in the cool season. The Applied Meteorology Unit (AMU) was tasked to develop tools that make short-range forecasts of peak winds at tower sites of operational interest in support of ELV and Shuttle launches and Shuttle landings in the cool season months of October – April.

The data used for this task were from all towers in the Kennedy Space Center/Cape Canaveral Air Force Station (KSC/CCAFS) wind tower network for all months in the period 1995 – 2001. Specifically, the 5-minute average and peak speeds and directions were analyzed for tool development. Erroneous wind observations were removed from the data set prior to analysis using five quality control (QC) routines developed specifically for the KSC/CCAFS wind tower network data. Only a small percentage of the data were flagged as erroneous.

The first step in developing a peak-wind forecasting tool was to develop climatologies of the speeds and directions. The data were stratified by tower number, height and month, then by hour, direction, and direction/hour. The means and standard deviations (σ) of the peak and average speeds were calculated, and the numbers of observations used in the calculations were tabulated. The hourly climatologies showed a diurnal trend with stronger winds in the afternoon hours and a close relationship between the average and the peak winds, but the σ values were quite large. Large variability was also evident in the other climatologies. This was an indication that the climatologies were smoothed values of highly variable data, and may not be useful in a forecast tool for peak winds.

The relationship between the 5-minute average and peak winds was examined in the next step. The distributions of peak speeds for each average speed could be used to calculate the probability of exceeding a specific peak speed given the average speed. The probability density functions (PDFs) of the peak speeds appeared to have a distribution other than Gaussian, so tests were done to determine the appropriate theoretical distribution. Qualitative and quantitative tests indicated that the Weibull distribution best described the empirical PDFs. The Weibull parameters of mu, scale, and shape (analogous to mean and σ for a Gaussian distribution) for each average speed value were estimated from the observed PDFs. An increasing trend with speed was evident in the parameters except for the higher average speeds that had < 600 observations in the stratified data sets. We assumed initially that the higher-speed parameters were erroneous and the trend of the lower-speed parameters could be extrapolated to estimate the parameters for the higher speeds with few or no observations. The trends were modeled with polynomial regression equations, and the parameters for the higher average speeds were estimated with those equations. The results of tests to check the validity of the modeled parameters were ambiguous at best. The conclusion is that the PDFs for the speeds with < 600 observations can not be modeled with confidence and should not be used for the development of an operational product.

Based on the analyses of the climatologies and distributions, the main conclusion is that the stratifications and methods used in this study are unable to capture the physical mechanisms that caused peak winds so they can be used in the development of a prognostic tool. The phenomena responsible for high average and peak speeds include synoptic frontal passages, convective outflow boundaries, and the mixing down of high momentum air from aloft. However, stratifying the data by phenomenon would be difficult and time-consuming, and may result in data sets with too few observations from which to develop valid forecast tools. Three previous studies attempted to produce cool-season peak wind forecasting techniques for operations at KSC/CCAFS without success. They found the development of such a tool to be difficult, and the results from this task underscore that difficulty.

Although a forecast tool was not developed, the output from the analyses done in this task could be useful in operations. The climatologies and peak-speed PDFs for average winds with > 600 observations are valid analyses based on the historical behavior of the winds. Forecasters at the 45 WS and SMG have indicated that one or both of these products would be useful in their analysis and forecasting of winds. These products are not prognostic in nature. However, the climatologies can provide the forecasters with information about the average behavior of the speeds and directions during time periods of future launches, and the PDFs can be used to estimate the probability of meeting or exceeding a certain peak speed based on the forecast of an average speed value.

Table of Contents

Executive Summary.....	iii
List of Figures	v
List of Tables.....	vi
1. Introduction	1
1.1. Operational Issues.....	2
1.2. Previous Work	2
1.3. AMU Study.....	3
2. Data	4
2.1. Wind Tower Data	4
2.2. Data Quality Control.....	5
3. Climatology	8
3.1. Hourly Climatology	8
3.2. Directional Climatology	10
3.3. Directional/Hourly Climatology	12
3.4. Climatology as a Predictor.....	14
3.5. Climatology Product.....	14
4. Peak Wind Speed Distributions	16
4.1. Empirical Distributions.....	16
4.2. Theoretical Distribution Determination	17
4.3. Estimation of Empirical and Modeled Weibull Parameters.....	18
4.4. Analysis of Modeled Distributions	21
5. Conclusions	27
5.1. Summary and Analysis of Results	27
5.2. Operational Products.....	28
5.3. Future Work.....	29
References	31
List of Acronyms	32

List of Figures

Figure 1.	A map showing the locations of the wind towers used in the task.....	1
Figure 2.	Mean hourly wind speed (kts) for March for Tower 0393 at 60 ft.....	9
Figure 3.	Mean winds speeds (kts) as a function of 10° wind direction bins for March for Tower 0393 at 60 ft. The values on the x-axis represent the upper range of the direction-bins.	10
Figure 4.	The number of observations used in the mean and σ calculations as a function of 10° wind direction bins for March for Tower 0393 at 60 ft.....	11
Figure 5.	Mean hourly wind speed (kts) for a NNW wind (316 - 360°) in March for Tower 0393 at 60 ft.....	12
Figure 6.	The number of observations used in the mean and σ calculations as a function of hour for NNW winds (316 - 360°) in March for Tower 0393 at 60 ft.	13
Figure 7.	Time series of 5-minute peak wind observations in the 48-hour period from 0000 UTC 1 January to 0000 UTC 3 January 1996 (gray line) overlaid with the hourly climatology values for January (black line) from Tower 0036 at 90 ft.....	14
Figure 8.	The number of 5-minute average wind speed observations as a function of hour for WNW winds (271 - 315°) in March, April, and May for Tower 0393 at 60 ft.....	15
Figure 9.	The empirical PDFs of the January peak wind speed distributions associated with each 5-min average wind speed (see legend) from 1 - 25 kts for Tower 0397 at 60 ft.	17
Figure 10.	The Weibull mu, scale and shape parameter values for the peak wind speed PDFs (see Figure 9) based on the January 5-min average wind speeds from 1 - 30 kts for Tower 0397 at 60 ft.	19
Figure 11.	The observed (thin lines) and modeled (thick lines) Weibull scale, mu, and shape parameter values for the peak wind speed PDFs based on the January 5-min average wind speeds from 1 - 30 kts at Tower 0397.	20
Figure 12.	Modeled PDFs of the January peak wind speed distributions associated with each 5-minute average wind speed (see legend) from 1 - 30 kts at Tower 0397/60 ft.....	21
Figure 13.	The standard errors of the empirical Weibull mu, scale and shape parameter values in Figure 10.	22
Figure 14.	Chart of the differences between two standard errors of the observed parameters and the difference between the empirical and modeled parameter values.	23
Figure 15.	The modeled and empirical gust factors for Tower 0397 at 60 ft in January.....	24
Figure 16.	The estimated Weibull PDFs of the January peak wind speed distributions associated with each 5-minute average wind speed (see legend) from 2 - 18 kts for Tower 0397 at 60 ft.	25
Figure 17.	The probability curves for the estimated Weibull PDFs in Figure 16.....	26

List of Tables

Table 1.	The towers and heights at which forecasts for peak winds will be made and the associated launch operation.	1
Table 2.	Towers with redundant sensors and information about the location of the sensors relative to the towers. Each side of the tower is given a distinct number.....	5
Table 3.	Parameter settings for the two limit-check QC routines. Observations were flagged if they were lower than the minimum threshold, higher than the maximum threshold, or more than the specified number of standard deviations from the mean.	6
Table 4.	Algorithm for editing anomalous peak wind speeds. Given the average wind speed range in the left column, if the corresponding ratio in the right column is exceeded, the peak wind speed is flagged.....	6
Table 5.	Numbers and percentages of the observations in the data set affected by the peak/average wind speed ratio QC. The percent values in the far right column were calculated with the equation: $100 * \text{Number Flagged} / \text{Number of Observations}$	7

1. Introduction

The peak winds are an important forecast element for both the Space Shuttle and Expendable Launch Vehicle (ELV) programs. As defined in the Shuttle Flight Rules (FR) and the Launch Commit Criteria (LCC), each vehicle is assigned certain peak wind thresholds that cannot be exceeded in order to ensure the safety of that vehicle during launch and landing operations. The 45th Weather Squadron (45 WS) and the Spaceflight Meteorology Group (SMG) indicate that peak winds are challenging to forecast, particularly in the cool season. The Applied Meteorology Unit (AMU) was tasked to develop tools that make short-range forecasts of peak winds at the tower sites shown in Table 1 in support of ELV and Shuttle launches and Shuttle landings in the cool season months of October – April. A map of the tower locations is in Figure 1.

Table 1. The towers and heights at which forecasts for peak winds will be made and the associated launch operation.			
<i>Launch Operation</i>	<i>Tower(s)</i>	<i>Primary Height (ft)</i>	<i>Backup Height (ft)</i>
Shuttle	0393/0394 (<i>NW and SE of SLC 39A, resp.</i>) 0397/0398 (<i>NW and SE of SLC 39B, resp.</i>)	60	N/A
Shuttle (<i>landing</i>)	0511 / 0512 / 0513 313	30 492	N/A N/A
Atlas	0036	90	N/A
Delta	2	90	54
Titan	110	162	54

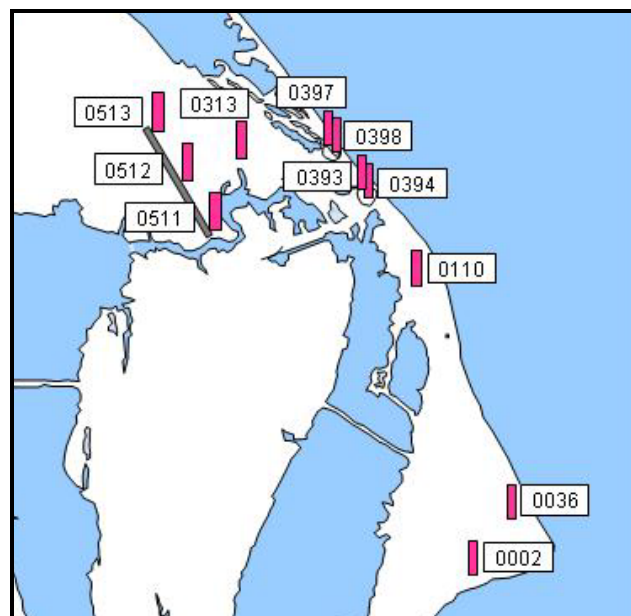


Figure 1. A map showing the locations of the wind towers used in the task.

1.1. Operational Issues

Launch vehicles are exposed to the weather from the time their service tower is removed through launch, which could be up to 10 hours. If a launch is scrubbed, the vehicle is exposed for a longer period as it must be de-tanked before its service structure is put back in place. During this time period, the vehicle is susceptible to damage from winds that exceed the vehicle's tolerance threshold. Such winds could cause airborne debris to impact and damage the vehicle, or cause the vehicle to oscillate to the point that it damages support lines or makes contact with its supporting structure. As the Shuttle lands, crosswinds that exceed the operational threshold could cause damage to the orbiter. The results of such damage could be costly and catastrophic, and could also result in loss of human life.

Accurate forecasts of peak winds, therefore, are critical to protecting the health and safety of launch pad workers and astronauts as well as preventing financial losses due to delays and damage. Such forecasts are valuable to launch directors when deciding not only to launch but whether to continue with pre-launch procedures, and to flight directors who must decide whether to issue a GO for a Shuttle landing at the de-orbit burn decision time.

1.2. Previous Work

Several studies using Kennedy Space Center (KSC) / Cape Canaveral Air Force Station (CCAFS) wind tower network data have taken place to aid in determining the effects of winds on space vehicle design. One such study used one year of data from Tower 0313 to determine ratios of peak wind to average wind for different stratifications of average speed strength and stability, also known as the gust factor (McVehil and Camnitz 1969). The principle was that an average wind speed multiplied by the appropriate gust factor, which averaged ~ 1.5 , would produce a reasonable estimate of the expected peak wind. This technique was purely diagnostic: the peak wind estimate was associated with a concurrent average wind speed. To use as a prognostic tool, a forecaster must first make an average wind speed forecast, then multiply this value by the appropriate gust factor to estimate the peak wind at the forecast verification time. A modified version of this technique is currently used by SMG.

The desire for a prognostic tool brought about three research projects at the Air Force Institute of Technology (AFIT) to develop a reliable peak wind forecast method. In the first project, a neural network model was developed to predict peak winds at several launch pads and compared the model forecast to persistence (Storch 1999). The neural network performed similarly to persistence, and neither the network nor persistence showed good skill in predicting peak winds.

Cloys (2000) also employed a neural network to forecast peak winds at the 90' level of Tower 0036 at the Atlas ELV launch site. Forecasts from two configurations of a neural network were compared to persistence, conditional climatology, and random forecasts. The neural network performed worse than persistence, although at some times toward the end of the forecast period it performed similarly to persistence. None of the methods in the analysis performed well enough to be used in operations.

Finally, Coleman (2000) developed a conditional climatology of cool season winds at several of the towers used for launch forecasts. The wind data from each tower and height were stratified by month, hour, direction and speed. The probabilities of occurrence of specific speeds and directions based on the current observation were calculated for every hour out to 8 hours. The conditional climatology values were evaluated for their ability to forecast peak winds through tests with independent data. The results indicated the conditional climatologies did not perform well and were not recommended for use in operations.

None of the three AFIT studies described in the preceding paragraphs produced the desired result of an operational product to aid in peak wind forecasting. They may have been unsuccessful due to selection of improper methodologies, incorrect or not enough data, or the difficulty of predicting wind gusts. AFIT students also have only a short time available to conduct and complete thesis research, which may not be enough time to attempt to solve such a difficult forecasting issue. Nonetheless, the fact that no useful products were developed from these three studies underscores the difficulty in determining a method to predict peak winds.

1.3. AMU Study

Given the absence of successful peak-wind forecasting studies, the AMU had little guidance in determining appropriate predictors and statistical methods. Attempts were made to use wind tower peak speed climatologies and past observations to forecast peak wind speeds at individual towers. However, almost no correlations were found between the climatological values/past observations and the peak speeds to be forecasted. The conclusion from these attempts was that the physical mechanisms generating wind gusts are complex and difficult, if not impossible, to discern from the wind observations alone. Through internal discussions and meetings with customers, it was decided that data from other towers and other data types were needed in the method to develop a peak speed forecast tool for each tower. Since some models contain equations that attempt to describe the physics involved in the production of gusts, the use of a high-resolution model was also considered as a possible component of a peak wind forecasting tool. However, these options could not be pursued due to task time constraints.

Therefore, this study focused on the behavior of the peak winds at each sensor in Table 1 based on month, hour, direction, and 5-minute average wind speed. Section 2 describes the data used in this study including period of record, locations, and quality control. Section 3 shows the results of wind speed and direction climatologies, and Section 4 discusses the procedures used to determine the peak wind distribution by average wind speed and shows the results. The final conclusions are assembled in Section 5.

2. Data

Three data types were collected for this task: hourly surface observations from the Air Force Combat Climatology Center (AFCCC), hourly buoy data from the National Data Buoy Center (NDBC) web site, and data from all wind towers in the KSC/CCAFS network from the Range Technical Services Contractor, Computer Sciences Raytheon (CSR). Only the wind tower network data were analyzed in this phase of the task, but the other data were collected for the possibility of incorporating them in the development of a more complex peak wind forecasting tool in a future phase.

2.1. Wind Tower Data

Data were collected from all towers in the network over the period 1995 – 2001 for all months. Data before 1995 were not used because of a known noise problem in the archived peak winds that was fixed in late 1994 (William Roeder, 45 WS, personal communication). The analysis concentrated on cool-season data from the months October through April since this was identified by the forecasters as being the most difficult time period in which to forecast peak winds. Forecasting peak winds is difficult in the warm season as well, but the wind speeds are usually far below the operational thresholds. The data set consists of the year/month/day/hour/minute and height of the observations. The time resolution of the data is 5 minutes. The meteorological variables in the data set include the

- Temperature and dew point temperature in degrees Celsius,
- 5-minute average and 5-minute peak wind speeds in meters per second,
- 5-minute average and 5-minute peak wind direction in degrees,
- Deviation of the 5-minute average wind direction in degrees, and
- Relative humidity in percent.

The wind speed and direction data were sampled every second. The 5-minute average is the mean of all 600 1-second observations in the 5-minute period. The peak wind is the maximum 1-second speed in the 5-minute period and its associated direction. Before processing, the temperatures were converted to degrees Fahrenheit with the equation

$$^{\circ}\text{F} = 1.8 * ^{\circ}\text{C} + 32,$$

and the wind speeds were converted to knots (kts) with the equation

$$\text{Knots} = 1.9424 * \text{ms}^{-1}.$$

Only data from the towers in Table 1 were processed and analyzed for this task. Several of the towers in Table 1 have sensors on two sides. Each side has its own number designation as shown in Table 2. The redundant sensors at these towers were added in response to the effect of obstructed wind flow around the tower on the downwind sensor. They were also added so that one sensor could be used as a backup for the other in case of failure. Only data from the windward side of each tower are displayed to the forecasters, but data from both sensors at each tower were in the data set and continue to be collected and archived. The data from both sensors at the redundant towers were processed and analyzed as separate sensors.

Table 2. Towers with redundant sensors and information about the location of the sensors relative to the towers. Each side of the tower is given a distinct number.

<i>Tower Number</i>	<i>Side: Number</i>
313	Northeast: 3131 Southwest: 3132
36	Sensors at top of tower
2	Northwest: 0020 Southeast: 0021
110	Northwest: 1101 Southeast: 1102

2.2. Data Quality Control

Erroneous observations were removed from the data set prior to analysis. Five quality control (QC) routines developed by Dr. Fred Riewe of ENSCO, Inc. specifically for the KSC/CCAFS wind tower network data were used to QC the data:

- An unrealistic value check (e.g. wind speed < 0),
- A standard deviation (σ) check (e.g. temperature not within 10σ of mean),
- A peak-to-average wind speed ratio check in which the peak wind must be within a specified factor of the average wind speed (factor value dependent on average speed),
- A vertical consistency check between sensor levels at each individual tower, and
- A temporal consistency check for each individual sensor.

Only a small percentage of the data were flagged as erroneous by these QC routines: from 0.6 to 2.1% per tower and month, which resulted in a large set of good quality data for analysis and forecast-tool development. A short description of each routine follows.

2.2.1. Limit Checks

The first two QC routines mentioned in the previous section imposed range limits on the data. In the first, all data with unrealistic values were removed from the data set. The unrealistic-value thresholds were determined through consultations with operational forecasters. If a value exceeded the maximum threshold or dropped below the minimum threshold, it was flagged as erroneous. The minimum and maximum threshold values used in this QC algorithm are shown in Table 3.

The second routine performed a standard deviation check specific to each tower, month, and time of day. For all years in the data set for a given tower, the data were first stratified by month to ensure that the subtle seasonal changes in each month were not contaminated by those in another month. Then each month was stratified by each 5-minute time in the month. The data were not stratified by day of the month to ensure that the sample size used to calculate the means and standard deviations was large enough. For a standard month of 30 days, a maximum of 210 observations were available for the calculations (30 5-minute times x 7 years) assuming no missing data. An individual observation was flagged as erroneous if it differed from the mean by more than the number of standard deviations shown in the last column in Table 3. Wind direction was the only meteorological variable not subjected to the standard deviation check.

Table 3. Parameter settings for the two limit-check QC routines. Observations were flagged if they were lower than the minimum threshold, higher than the maximum threshold, or more than the specified number of standard deviations from the mean.

<i>Meteorological Variable</i>	<i>Data Value Ranges</i>		<i># Standard Deviations</i>
	<i>Min</i>	<i>Max</i>	
Temperature	-15 F	105 F	5
Dew Point Temperature	0 F	95 F	5
Average Wind:			
Speed	0 kts	115 kts	10
Direction	0°	360°	—
Peak Wind:			
Speed	0 kts	135 kts	10
Direction	0°	360°	—
Pressure	960 mb	1040 mb	5

2.2.2. Peak/Average Wind Speed Ratio

After Dr. Riewe examined the data that had been flagged by the limit checks, he noticed through a manual inspection that the data still contained invalid peak wind speed values. He calculated the ratio of peak to average speed and plotted the number of occurrences of each ratio for each average wind speed. He determined that the higher ratios were the result of erroneously high peak speeds, and developed an algorithm that flagged these erroneous peak speeds. The values used in the algorithm are shown in Table 4.

Table 4. Algorithm for editing anomalous peak wind speeds. Given the average wind speed range in the left column, if the corresponding ratio in the right column is exceeded, the peak wind speed is flagged.

<i>Average Wind Speed (kts)</i>	<i>Maximum Allowed Value of Peak-to-Average Wind Speed Ratio</i>
< 2	No limit
2	10
3 to 8	$2.6 + 0.16 * \text{average wind speed}$
> 8	2.5 for levels below 50 ft 2.0 for levels 50 ft and above

There was some concern this algorithm would flag legitimate high peak values. If this happened, the climatology and distribution estimates would be invalid. In particular, the tails of the peak speed distributions could be eroded or eliminated, resulting in incorrect probability values of meeting or exceeding specified peak speeds. Of particular concern was the flagging of higher peak speeds associated with higher average speeds. The analysis in Section 4 of this report showed that the number of average speed observations greater than approximately 15 kts dropped dramatically to the point that accurate distributions could not be estimated. Tests were done to determine if this QC algorithm contributed significantly to that drop in observations. Calculations were done to determine how many observations and what percentage of total data points were affected by this algorithm. The results are shown in Table 5.

Table 5. Numbers and percentages of the observations in the data set affected by the peak/average wind speed ratio QC. The percent values in the far right column were calculated with the equation: 100 * Number Flagged/Number of Observations.

<i>Data Range</i>	<i>Number of Observations</i>	<i>Number Flagged</i>	<i>Percent Flagged</i>
Total Observations in Data Set Checked by Algorithm	11 833 977	10 343	0.09%
Average Speeds in Data Set > 15 kts and ≤ 20 kts	686 901	338	0.05%
Average Speeds in Data Set > 20 kts	209 906	86	0.04%

The first row in Table 5 shows the results for the entire data set, all observations from all towers and months. Less than 1/10 of 1% of peak winds associated with any average speed were flagged. The next two rows show the results for two subsets of the total data set: average speeds > 15 to 20 kts and > 20 kts. Again, these values are for all months and towers combined. The numbers of flagged peak speeds are so small that it is highly unlikely that this QC algorithm contributed to the drop in observations beyond 15 kts average speed seen in the analyses.

2.2.3. Vertical Consistency

A wind tower network data QC algorithm for different heights at a given time exists and is used in the present Meteorological And Range Safety Support (MARSS) system. The algorithm compares a wind observation at a certain height to the vector difference of winds at levels above and below that observation. The vector difference ΔV_i for the i th level is computed from the u - and v -components at the heights directly above and below using the equations

$$\Delta u_i = \frac{1}{2}(u_{i-1} + u_{i+1}) - u_i,$$

$$\Delta v_i = \frac{1}{2}(v_{i-1} + v_{i+1}) - v_i, \text{ and}$$

$$\Delta V_i = [(\Delta u_i)^2 + (\Delta v_i)^2]^{1/2}.$$

If wind data were missing at level $i-1$ or $i+1$, then the algorithm used the next lower or higher level, respectively. If there was no next lower or next higher level, the observation at level i was not QC'd. The lowest and highest levels at a tower were not QC'd. The wind speed and direction were flagged as erroneous when $\Delta V_i \geq 15$ kts.

2.2.4. Temporal Consistency

Because the vertical check required data at heights both above and below the level being analyzed, much of the tower data could not be evaluated. However, there was no such limitation on temporal data checking. Such a temporal check exists in MARSS and uses the same algorithm as the vertical check, but the subscripts $i-1$, i , and $i+1$ correspond to data at the three 5-minute time intervals centered on the data being evaluated. If values were missing at times $i-1$ or $i+1$, the algorithm used the next earlier or later value, respectively. If the next earlier or later time was missing, the observation at time i was not QC'd. As with the vertical check, the wind speed and direction were flagged as erroneous when $\Delta V_i \geq 15$ kts.

3. Climatology

The first step in understanding the behavior of the winds was to develop climatologies of the speeds and directions. It was expected that these values would also help determine the optimal forecast model and be used for input to that model. The climatologies consisted of wind speed (peak and average) means and standard deviations calculated with the commercial-off-the-shelf statistical software package S-PLUS[®] (Insightful Corporation 2000). The data were stratified first by tower/height combination and month, then by three other ways prior to the calculations:

- By hour,
- By direction in 10° bins, and
- By direction in 45° bins and hour.

In addition to calculating the mean and σ of the wind speeds, the number of observations used to calculate these variables were tabulated. The results were then displayed in Microsoft[®] Excel pivot charts. These charts allowed flexibility and speed in displaying the wind speed data by hour, direction, month, and variable (mean, σ , number of observations).

3.1. Hourly Climatology

For this climatology, the hourly mean and σ of the 5-minute average and 5-minute peak winds were calculated for each month and tower/height combination. The hourly values were calculated by using the 12 5-minute values in each hour for each day of the month from every year in the data set. The March hourly climatologies for Tower 0393 at 60 ft, located just northwest of Space Launch Complex (SLC) 39A (Shuttle), are shown in Figure 2. The total number of possible observations in March was 62 496 (*12 obs/hr x 24 hrs/day x 31 days/March x 7 Marches*); and the total number of possible observations per hour was 2604 (*62 496 obs / 24 hrs*). The actual number of observations used to calculate the values was slightly lower due to missing and QC-flagged data. The number of observations for each hourly calculation in Figure 2 ranged from 2300 – 2400, which was a sufficiently large sample from which to calculate reliable climatologies.

The main feature seen in Figure 2 is the diurnal trend in both the mean peak and average wind speeds. While these are the results for Tower 0393, this diurnal trend was evident in all other towers as well. The local sunrise in March is between 1100 - 1200 UTC (0600 - 0700 EST), and sunset is between 2300 - 2400 UTC (1800 – 1900 EST). An increase in mean speed was apparent in the data after sunrise, as was the decrease in the late afternoon to evening hours. The increase at sunrise was likely due to the mixing down of higher momentum winds aloft by the convective updrafts and downdrafts created by daytime heating. Also noteworthy was the close correlation between the mean peak and average wind speeds. This helped confirm the validity of the gust factor forecast method used at SMG and that it should be used as a benchmark to test the added value of any new peak-wind forecasting technique.

The σ curves indicated a large variability in the winds of 6 - 7 kts for the peak speeds and 4 - 5 kts for the average speeds. Such large variability indicated that the means might merely be smoothed low frequency values of high frequency and highly variable data. While the smoothed mean values may be useful in revealing overall diurnal trends, they would be less useful in forecasting the value of a peak wind on any given day. This was the first indication that climatology might not be a good predictor for peak winds, and that development of a forecast tool would be challenging due to the large variability.

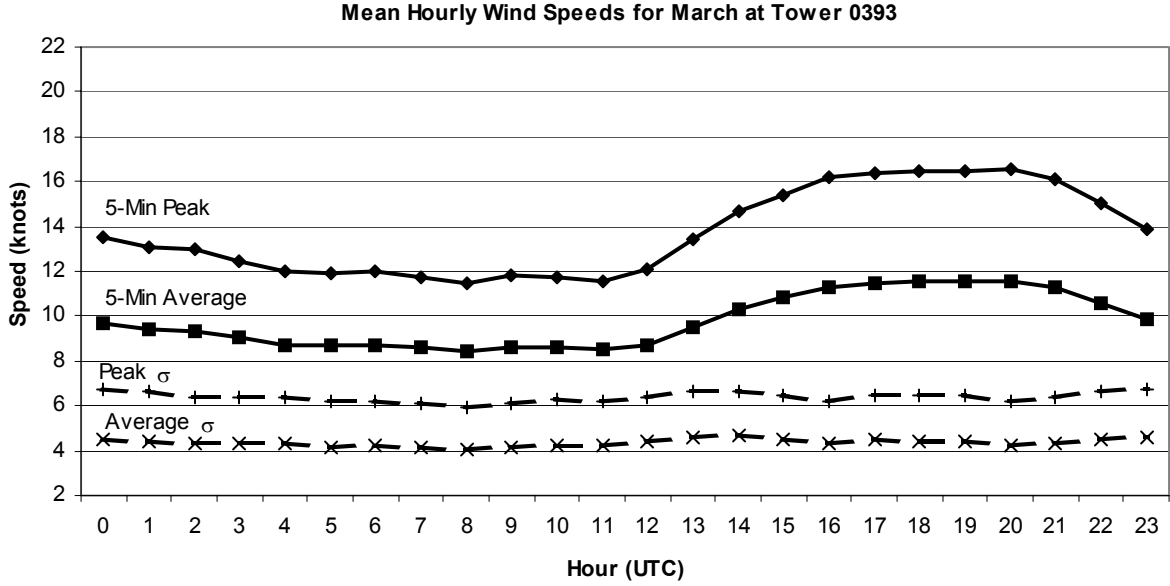


Figure 2. Mean hourly wind speed (kts) for March for Tower 0393 at 60 ft. The first (top) solid line is the hourly mean of the 5-minute peak wind speed, the second solid line is the mean of the 5-minute average wind speed, the first dashed line is the standard deviation (σ) of the peak speed, and the second dashed line is the σ of the average speed.

3.2. Directional Climatology

This climatology was calculated to determine if there was a monthly pattern in direction for stronger or weaker winds and a preferred monthly direction based on the number of observations in each direction bin. The mean and σ of the 5-minute average and 5-minute peak winds were calculated for 10° direction bins. The directional climatology in March for Tower 0393 at 60 ft is shown in Figure 3. It is difficult to discern any trend in wind speed with direction, but it is apparent in Figure 3 that the strongest speeds were from the NNW (340 - 360°). Other months showed similar results, with some preference for stronger winds from a particular direction. The same chart for October (not shown) shows a peak from the NNW, but also a broad easterly peak from 40 – 110°. Each month showed slightly different characteristics, but no obvious pattern. Note that the close correlation between the mean peak and average wind speeds found in Figure 2 is present in Figure 3, as are the large σ values.

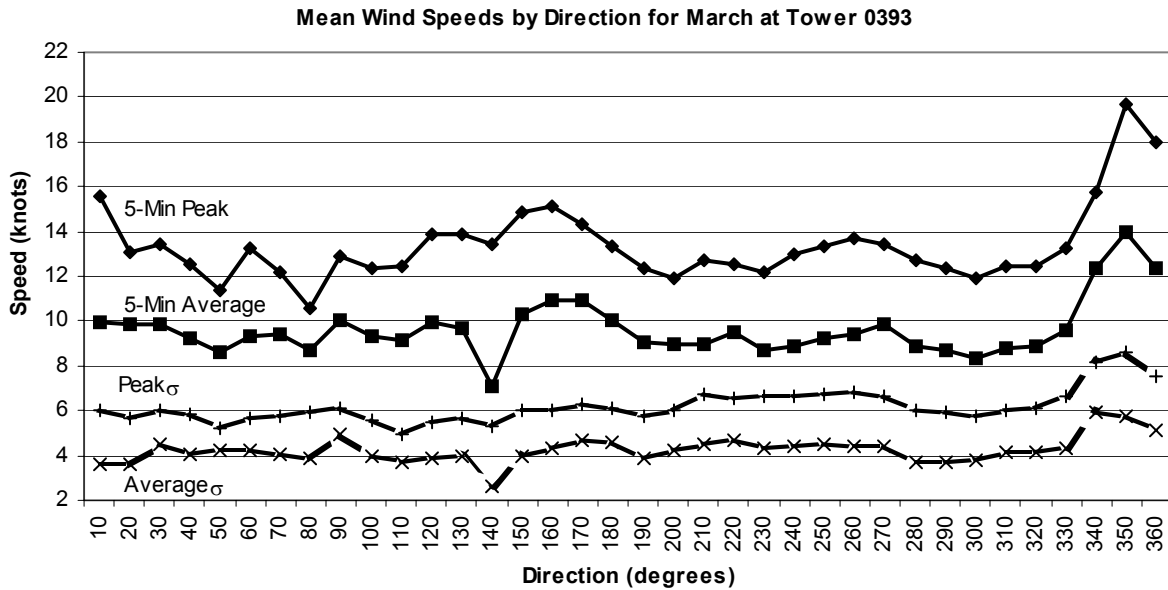


Figure 3. Mean winds speeds (kts) as a function of 10° wind direction bins for March for Tower 0393 at 60 ft. The values on the x-axis represent the upper range of the direction-bins. The first (top) solid line is the hourly mean of the 5-minute peak wind speed, the second solid line is the mean of the 5-minute average wind speed, the first dashed line is the standard deviation (σ) of the peak speed, and the second dashed line is the σ of the average speed.

The number of peak and average wind speed observations used in the calculations for Figure 3 are shown in Figure 4. This climatology was used to reveal any predominant wind direction(s) for each month. Along with the maximum in mean speeds from the NNW, there was also a maximum in the number of observations from these directions. Note the broad peak from 110 – 180°, and the anomalous drop in observations within that peak at 130 - 150°. Since Tower 0393 is located just to the NW of launch complex 39A, the drop in the number of SE wind observations is likely caused by the obstruction of flow around the launch pad just to the SE of the tower. This drop in the number of SE wind observations was not seen in the data from Tower 0394, which is located SE of the pad. However, there was a similar drop in NW wind observations from 310 – 330° at Tower 0394 in March (not shown). Note in Figure 3 the drop in magnitude of the mean and σ of the 5-minute average winds from these directions. This result emphasizes the need for redundant sensors on opposite sides of a tower or launch complex for observations critical to launch decisions.

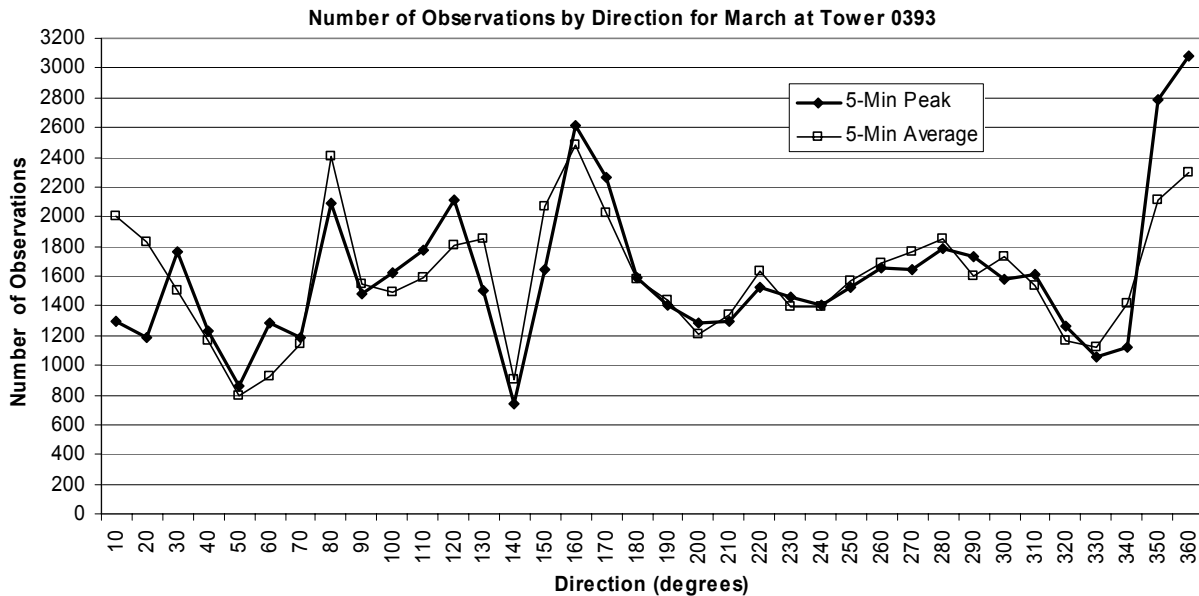


Figure 4. The number of observations used in the mean and σ calculations as a function of 10° wind direction bins for March for Tower 0393 at 60 ft. The values on the x-axis represent the upper range of the direction-bins. The thick line with diamonds is the count of the 5-minute peak winds, the thin line with boxes is the count of the 5-minute average winds.

The number of peak and average wind observations in Figure 4 were often close, but rarely equal for the same direction bin. In fact, there is a large difference in the numbers (~ 900) in the northerly winds between 350° and 20° . While there were times in which a peak wind was missing when an average speed was recorded, and vice versa, it is not likely that missing data is the cause of these large differences. In fact, there were only 72 cases out of over 57 000 in which one or the other wind observation was missing in the data represented by Figure 4. The large difference in the number of observations in each hour is probably the result of the binning process. The direction for each 5-minute average wind is averaged over the 5-minute period, while the peak wind direction is a 1-second value. Most often, the two values were different, with an average difference of $\sim 7^\circ$, which could cause them to be counted in different direction bins. Even with a difference of just 1° , e.g. 90° and 91° , the values could be put in adjacent direction bins, not the same bin. Larger differences would cause the values to be put in bins not adjacent to each other, which is probably what happened to the NNW - NNE winds in Figure 4. The surplus in peak wind observations at 350° and 360° was almost balanced by the surplus in average wind observations at 10° and 20° .

3.3. Directional/Hourly Climatology

This climatology was calculated to determine if there were preferential times of day during each month for stronger wind speeds from specific directions. The data were stratified first by direction bin, then hour. Several direction-bin increments were tested in combination with the 24 hourly bins. The direction increments had to be small enough to derive meaningful wind direction climatologies, yet large enough such that a sufficient number of observations were available to calculate dependable values. Eight 45°-direction bins provided the best balance.

Figure 5 shows the mean hourly wind speed parameters from the NNW (316 - 360°) in March for Tower 0393 at 60 ft. This direction bin was chosen to illustrate what time of day the maximum mean winds seen in Figure 3 were most likely to occur. There was an obvious diurnal trend in both mean and σ , large σ values, and a close correlation between the mean peak and average wind speeds. The mean speeds as a function of direction and time of day suggest that the strongest winds in March tended to be from the NNW (see Figures 3 and 4) at ~20 kts and occurred between 1800 and 0100 UTC (1300 – 2000 EST).

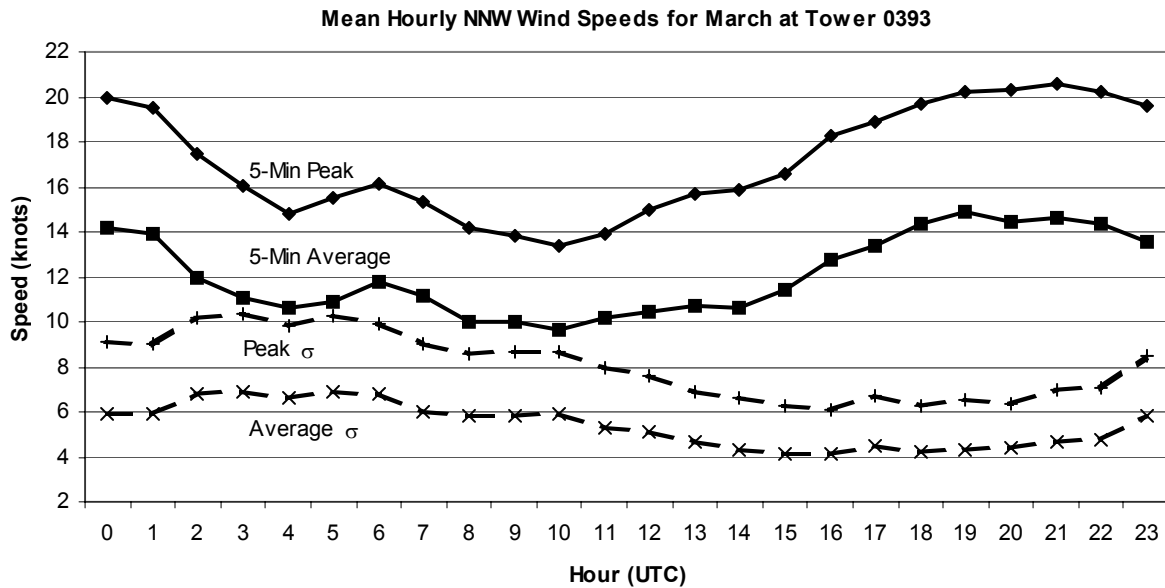


Figure 5. Mean hourly wind speed (kts) for a NNW wind (316 - 360°) in March for Tower 0393 at 60 ft. The first (top) solid line is the hourly mean of the 5-minute peak wind speed, the second solid line is the mean of the 5-minute average wind speed, the first dashed line is the standard deviation (σ) of the peak speed, and the second dashed line is the σ of the average speed.

The number of observations used to calculate the values in Figure 5 are shown in Figure 6. There is a broad peak centered on 1500 UTC, local mid-morning, showing that winds from the NNW were more likely to occur between local morning and noon in March. Note that in every hour there were fewer average wind observations (thin line) than peak wind observations (thick line). This is once again the result of the binning process as explained in Section 3.2. The graph of the number of wind observations from 1 - 45° (not shown) shows more average than peak wind observations, balancing out the deficit in the 316 - 360° bin shown in Figure 6.

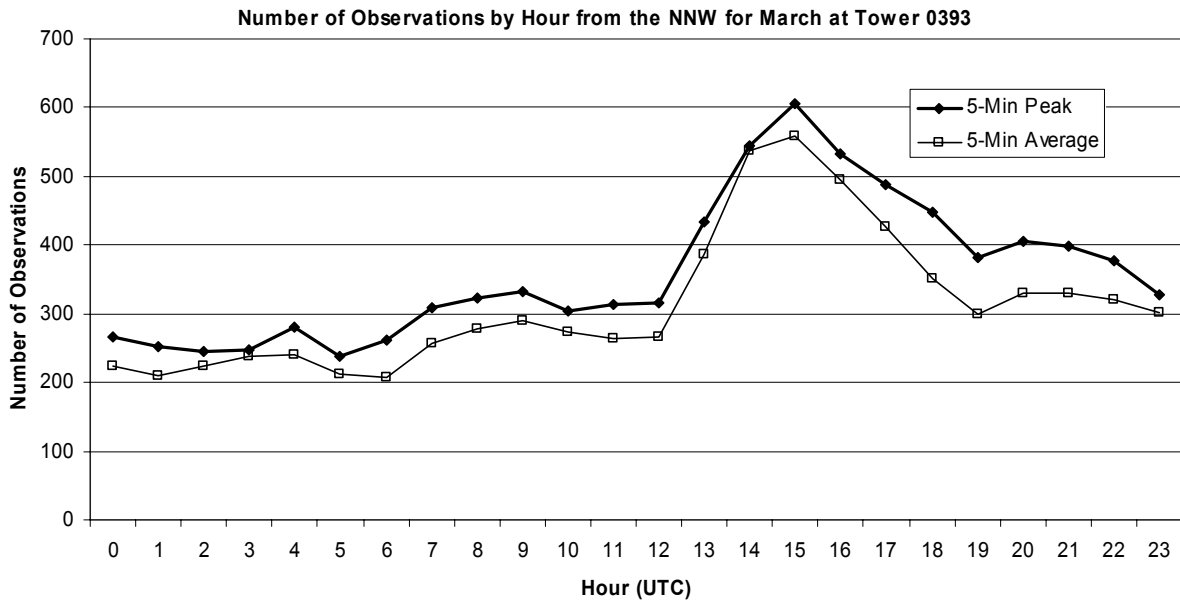


Figure 6. The number of observations used in the mean and σ calculations as a function of hour for NNW winds (316 - 360°) in March for Tower 0393 at 60 ft. The thick line with diamonds is the count of the 5-minute peak wind speeds, and the thin line with boxes is the count of the 5-minute average wind speeds.

3.4. Climatology as a Predictor

The climatologies described in the previous three sections provided some valuable information about the average behavior of the winds at each of the towers and heights of interest. Therefore, the peak wind climatology at each individual tower and height was examined for its utility in making short-term peak wind forecasts at that tower and height.

Figure 7 shows the 5-minute peak wind observations from Tower 0036 at 90 ft over a 48-hour period from 1 - 3 January 1996 overlaid with the January hourly peak speed climatology. Note the large variability in the time series of the peak wind observations and in the trends of the values. The climatology does show a diurnal variation in the speeds. However, it did not capture the observed ranges of values and their trends on these particular days because the climatology values were smoothed out in the averaging calculation. This helps to confirm the statement in Section 3.1 that the climatologies are smoothed low frequency values of high frequency and highly variable data. After examining several similar time series and reaching similar conclusions, the AMU concluded that the climatological values would be of limited use in the development of forecast equations.

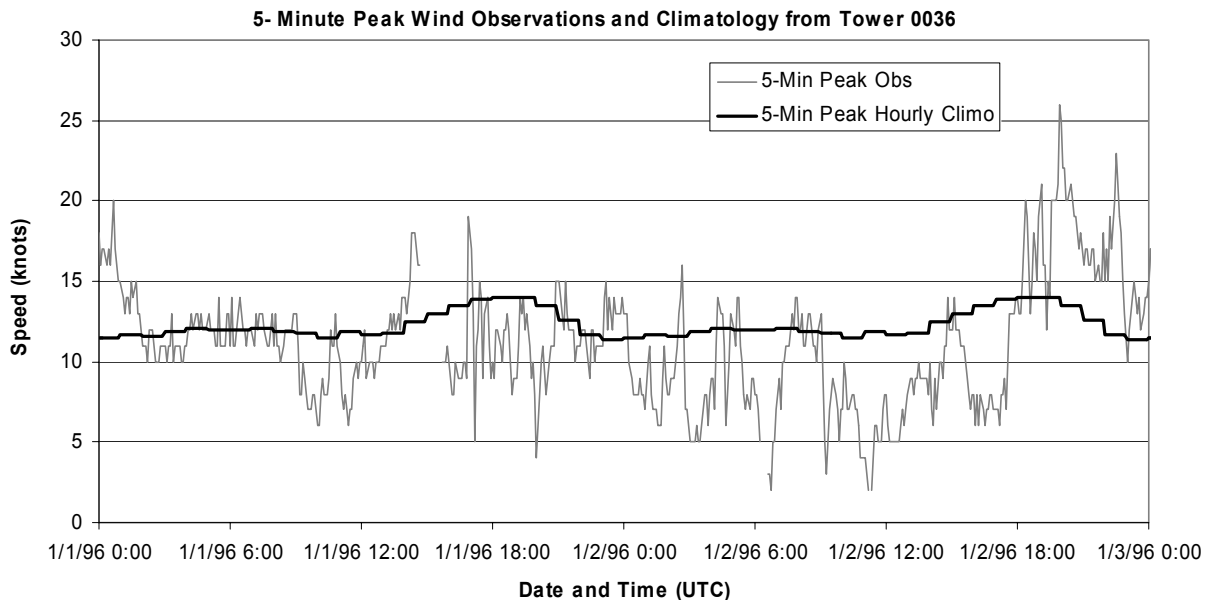


Figure 7. Time series of 5-minute peak wind observations in the 48-hour period from 0000 UTC 1 January to 0000 UTC 3 January 1996 (gray line) overlaid with the hourly climatology values for January (black line) from Tower 0036 at 90 ft.

3.5. Climatology Product

Although not likely to be useful elements in a short-term peak-wind forecasting tool, several forecasters indicated that the climatologies presented in Sections 3.1 – 3.3 revealed valuable information about the average behavior of the winds at the towers of interest. The charts of the peak and average wind speed means and standard deviations showed diurnal trends and relationships between the peak and average wind speeds, as well as preferred directions for the maximum speeds at specific times of day during specific months. Charts of the number of observations used to calculate the mean and σ revealed wind direction preferences per month and time of day.

As stated earlier, the climatologies were displayed in Microsoft® Excel pivot charts for analysis. A pivot chart allows the user to examine multi-dimensional data in different ways quickly through click-drag-drop techniques. For instance, instead of viewing the hourly number of observations from one direction and one month, as in Figure 6, the axes can be changed so that multiple months or directions can be viewed. Figure 8 shows the hourly change in the number of 5-minute average wind speed observations from the WNW (271 - 315°) at Tower 0393 for March, April, and May. The maximum in the number of observations in the early morning hours for each month may reflect the occurrence of land breezes. This is just one example of how the charts can be changed to display the parameters of interest. Because Excel is used by both the 45 WS and SMG, these climatology charts could be provided to each group for display and analysis.

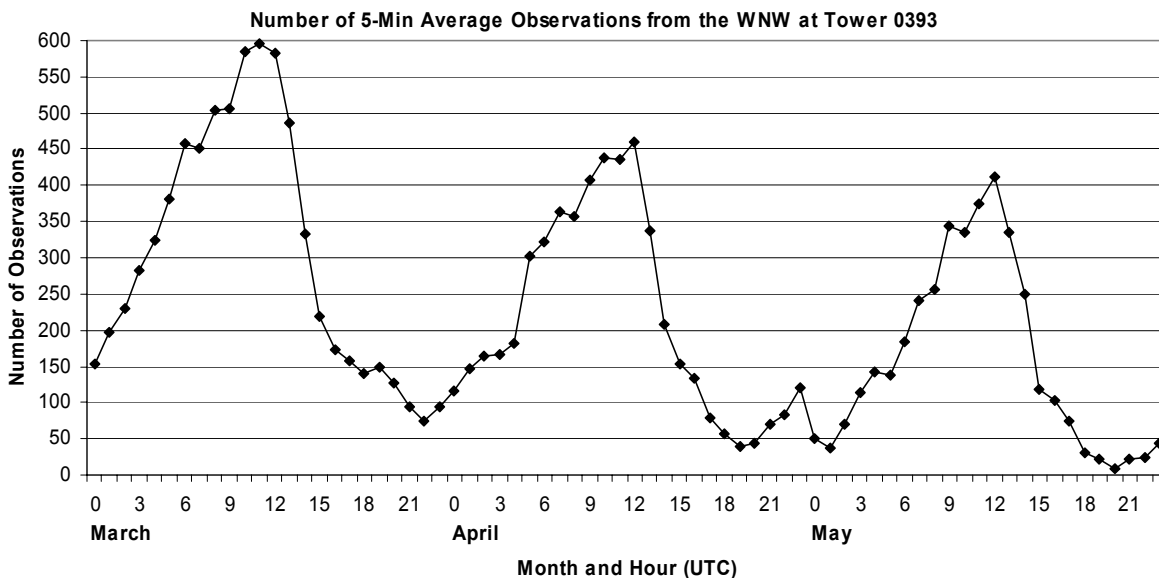


Figure 8. The number of 5-minute average wind speed observations as a function of hour for WNW winds (271 - 315°) in March, April, and May for Tower 0393 at 60 ft.

4. Peak Wind Speed Distributions

One of the goals of this task was to calculate the probability of meeting or exceeding a specific operational wind speed threshold. For every knot of 5-minute average wind speed, a range (or distribution) of peak winds were observed over the 7-year POR. The next step taken to understand the behavior of peak winds was to determine if a theoretical distribution could be used to describe these observed distributions. This served a two-fold purpose: 1) it yielded a greater understanding of how to determine peak speed behavior with average speed, and 2) produced a method that forecasters could use to determine the probability of meeting or exceeding a certain 5-minute peak speed given a 5-minute average wind speed.

4.1. Empirical Distributions

The first step in determining the appropriate theoretical distribution was to calculate the observed, or empirical, probability density functions (PDFs) over the observed 5-minute average wind speed spectrum for each month and tower/height combination. These PDFs were created using the S-PLUS[®] software. The calculation to create a PDF is straightforward. The number of observations for each individual peak speed in the distribution is divided by the total number of peak observations associated with each average wind speed. This produces a value that represents the fractional occurrence of each peak speed in the distribution. The sum of all the fractional numbers in the distribution is, therefore, 1. The results are plotted and the graph is called the PDF. The empirical PDFs for Tower 0397 in January are shown in Figure 9. Tower 0397 is located just northwest of SLC 39B and has a wind sensor at 60 ft. Each curve represents the range of peak wind values associated with a specific 5-min average speed (legend in Figure 9). The value on the y-axis is the fraction of events of a particular peak speed for a given 5-min average speed. To determine the probability of meeting or exceeding a certain peak value, one would integrate the area under the curve from the value of interest forward. Using values in Figure 9 as an example, the probability of exceeding 15 kts when the average speed is 10 kts (solid line with solid diamonds) is 0.34, or 34%.

One feature seen in Figure 9 is that the height and width of the PDFs decreased and increased, respectively, with increasing average speed in a consistent manner. When the average speed reached 19 kts, however, the PDFs no longer had a continuous shape nor continued the height/width trend of the previous PDFs. The number of observations used to calculate the PDFs for 19 kts and up was less than 600, with that number dropping quickly from 382 at 19 kts to 22 at 25 kts. The gray curves in Figure 9 show which PDFs were calculated with less than 600 samples. The number of observations for the average wind speeds decreased very rapidly with speed at higher wind speeds for all towers and heights.

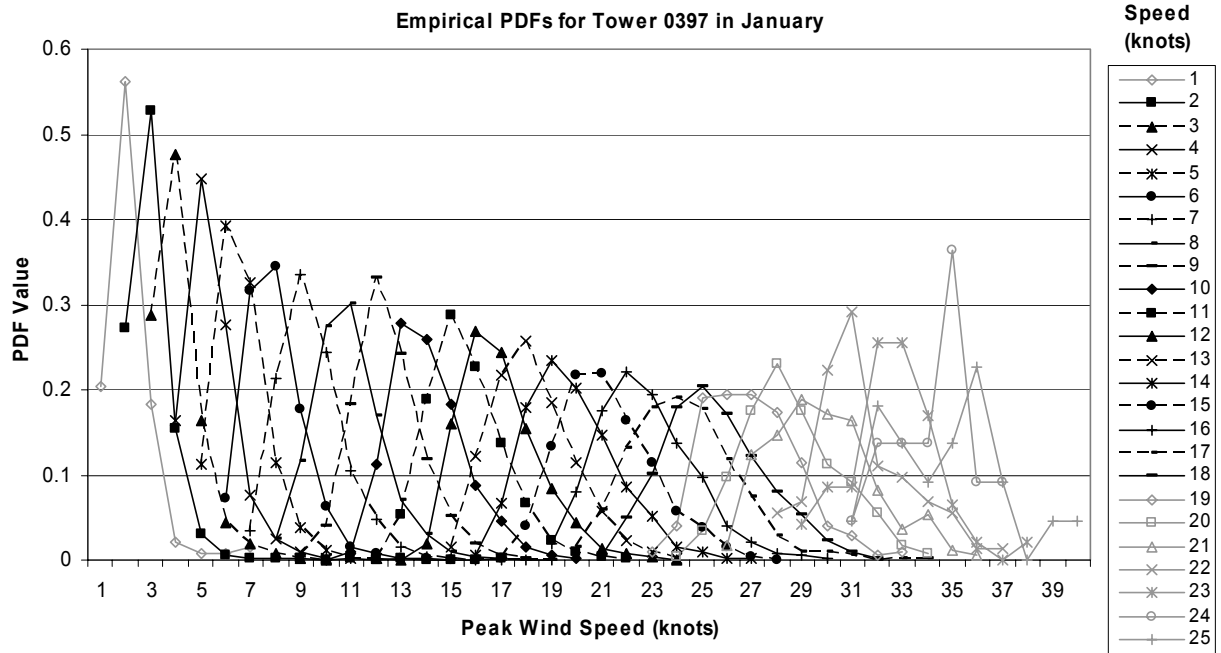


Figure 9. The empirical PDFs of the January peak wind speed distributions associated with each 5-min average wind speed (see legend) from 1 - 25 kts for Tower 0397 at 60 ft. The gray PDFs were calculated from distributions with less than 600 observations. The legend shows the 5-min average speeds associated with each PDF. The black PDFs alternate solid and dashed lines to make them easier to distinguish. The value on the y-axis is the fraction of events for a particular peak speed.

4.2. Theoretical Distribution Determination

There are several reasons for fitting theoretical distributions to empirical distributions defined in Wilks (1995), two of which applied in this study. The first was to smooth and interpolate over the variations in empirical distributions due to possible under-sampling of a specific peak gust. The second reason was to estimate probabilities of peak gusts associated with average wind speeds outside the range of the observations in the data sample. The assumption here is that the theoretical distribution would also represent the peak wind distributions for rarely or as-yet unobserved average wind speeds. Determining the validity of this assumption proved to be difficult for peak wind speeds.

The PDFs shown in Figure 9 and in the other towers were asymmetrical and, therefore, not Gaussian. They were also bounded on the left-hand side by the value of the average wind speed. Two possible theoretical distributions identified by Wilks (1995) for data with these characteristics are the gamma and Weibull distributions, although he identifies the Weibull distribution as being more widely used to model wind speeds. As this work began, Mr. Roeder of the 45 WS also suggested that the Weibull distribution would be most appropriate for the wind data. There is little support in the literature for using the gamma distribution for peak winds, but not so for the Weibull distribution. A subset of the many articles that support the use of the Weibull distribution for estimating wind gusts include Justus et al (1978), Van Der Auwera et al (1980), Tuller and Brett (1984), Pavia and O'Brien (1986), and Jagger et al (2001).

The results in the literature strongly advocated using the Weibull distribution. Still, both the gamma and Weibull distributions were compared to ensure that the most appropriate theoretical distribution was used to represent the wind speed data from the KSC/CCAFS wind tower network. This was done using built-in gamma and Weibull distribution estimation functions in S-PLUS. The peak wind observations for a given average wind speed (per tower/height) were input to the function. This function output the corresponding gamma and Weibull parameters that defined the best fit to the observed PDFs (Figure 9). Once the best-fit parameters were determined, they were input to another S-PLUS function that created ‘theoretical’ PDFs for both the gamma and Weibull distributions. The theoretical PDFs were plotted and compared qualitatively with the observed PDFs to determine which theoretical distribution fit the observed distribution best. This was done for all peak wind PDFs for every month at each tower and height. For PDFs with more than 600 observations, the Weibull fit to the observed PDFs was superior.

To confirm this result quantitatively, the Kolmogorov-Smirnov (K-S) test was conducted (Wilks 1995) for the empirical and theoretical Weibull distributions. This test calculates the largest difference (D) between the empirical and theoretical probabilities. If this number was sufficiently large, the null hypothesis that the sample was drawn from a population with a Weibull distribution could be rejected. In each case, D was sufficiently small that the null hypothesis could not be rejected at any level for the Weibull distribution. Neither theoretical distribution could be fit to the empirical PDFs created from much less than 600 observations (gray PDFs in Figure 9), which tended to be associated with average wind speeds greater than ~ 20 kts. There were not enough observations of those particular average wind speeds to create representative estimates of peak wind distributions for those speeds. However, wind speeds in this range are operationally significant and it would be beneficial to operational forecasters to know the expected range of peak speed values associated with them. The expectation was that the parameters for the Weibull distributions at these speeds could be estimated based on trends in the parameters of the lower speeds.

It should be noted here that the cutoff value of 600 observations is approximate, and not supported by any findings in the literature. An extensive manual data analysis revealed the cutoff number to produce a viable Weibull fit was approximately between 500 and 700. In one case, an average speed of 16 kts with 650 observations was fit successfully, while the following speed at 17 kts with 532 observations was not. This feature may be unique to the KSC/CCAFS wind tower network. Researchers following the methodology described here should be aware of this feature and examine their own data for its particular cutoff number.

4.3. Estimation of Empirical and Modeled Weibull Parameters

To determine the trends of the empirical Weibull parameters, the values had to be plotted versus average wind speed. Before the Weibull parameters were calculated, an offset had to be applied to the peak speeds associated with each average speed. The S-PLUS function that calculated the parameters assumed that the peak speed value on the left-hand side of the distribution was 0. The actual lower limit of the peak speeds in a distribution was the value of the associated average speed. For example, if the average wind was 15 kts, the lowest possible peak wind as measured in the KSC/CCAFS network was 15 kts if the winds were steady. The offset equation,

$$\text{Peak Offset} = \text{Peak Value} - (\text{Average Value} - 1),$$

was used for every peak value in each empirical distribution. This equation allowed for the possibility that a peak value could equal an average value in a steady wind. Using the 15-kt example, the probability of a 14-kt peak wind occurring would be 0, and the probability of a 15-kt peak wind would be greater than 0.

Figure 10 shows the Weibull parameters estimated from the empirical data shown in Figure 9. It includes the parameters for the average wind speeds up to 30 kts as that was the highest wind speed recorded at that tower in January, albeit only 5 times. Just as the mean and standard deviation describe a Gaussian distribution, the shape and scale parameters describe a Weibull distribution. The shape parameter determines the location of the maximum probability in the distribution. As the shape increases (decreases), the location of the maximum shifts to the right (left). The effect of the scale parameter is to stretch/compress the PDF horizontally, thereby also compressing/stretching it vertically. As the scale parameter goes to 0 the PDF appears as a spike, and as the scale parameter increases the PDF becomes more flat. The mu parameter is the mean peak value in the distribution calculated using scale and shape. All three parameters increase with average speed, although the shape increases more slowly. These values are consistent with the behavior of the PDF curves in Figure 9. The PDFs become shorter and wider as the scale increases, and the maximum PDF value shifts to the right in the distribution as the shape increases.

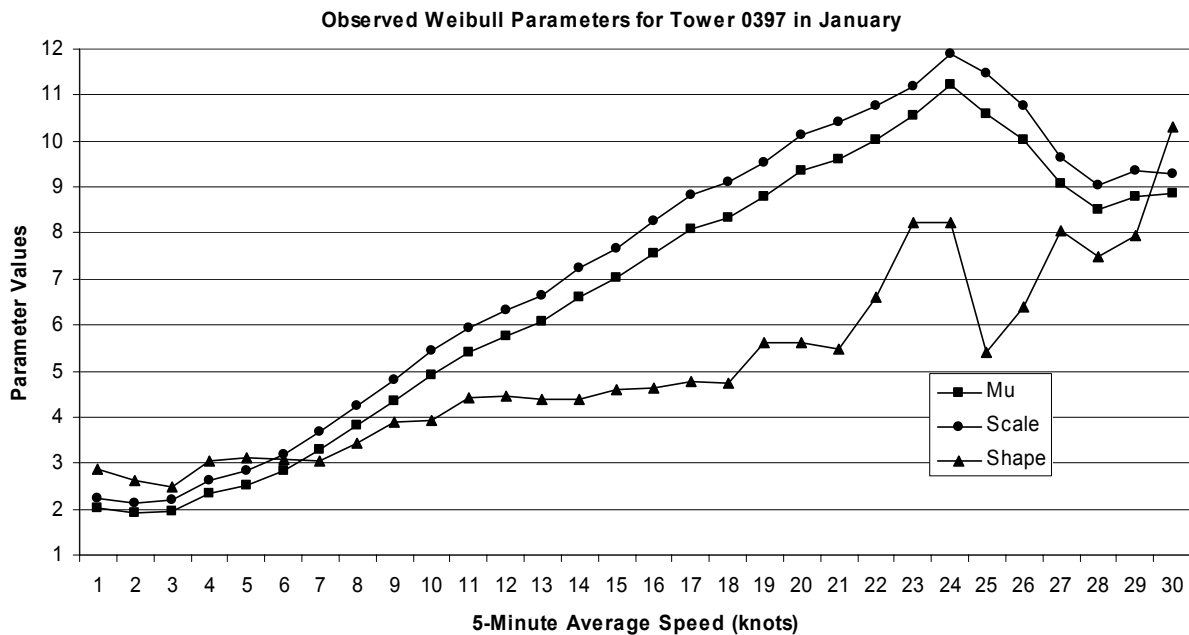


Figure 10. The Weibull mu, scale and shape parameter values for the peak wind speed PDFs (see Figure 9) based on the January 5-min average wind speeds from 1 - 30 kts for Tower 0397 at 60 ft.

The scale and mu parameter curves in Figure 10 have a continuous and increasing trend with average speed that could be modeled by a linear or curvilinear regression technique. The scale values at 1 and above 24 kts are questionable as they are inconsistent with this trend, but, as indicated in Figure 9, less than 600 observations were available to create the distributions at these speeds. As stated and shown previously, the PDFs for the average speeds 19 kts and higher did not follow the trends of the PDFs of lower speeds, possibly due to small sample sizes. The trend in the scale parameter is continuous through these higher speed values and appears valid. However, an abrupt change in the trend of the shape parameter occurs at 19 kts and above. This change occurs at the point where the sample size decreased below 600 and could indicate that any parameter values for such sample sizes are not reliable.

Another possibility is that the stronger winds were from different populations such as frontal passages, convective gust fronts, or high momentum air penetrating from above the inversion level. Their distributions may be something other than Weibull, but the sample sizes were too small to determine the actual distribution. Therefore, in order to estimate their theoretical PDFs it was assumed that their distributions were Weibull. Only the parameter values whose underlying sample size was ≥ 600 were used in the development of regression equations. The appropriate shape and scale parameters associated with each 5-min average speed, including those with small samples, would be modeled from the equations. The modeled Weibull parameters would then be used to create peak wind distributions for each average speed, from which probabilities of occurrence could be calculated.

In examining the parameters for all the towers, only the scale and mu parameters appeared to be continuous and more easily modeled. The shape parameter tended to be more erratic and difficult to model. Therefore, regression equations for the scale and mu parameters were tested, and shape would be calculated with the modeled scale and mu values. The results of testing linear and polynomial regression techniques indicated that a quadratic polynomial regression calculated the best estimate of the Weibull scale and mu parameters. The amount of variance in the parameter values explained by these polynomial equations (R^2) exceeded 98%. The equations were developed using the polynomial regression function in S-PLUS for each tower/height combination (18), each month in the cool season (7, October – April), and both the scale and mu parameters (2) for a total of 252 equations of the form

$$\text{Parameter} = Ax^2 + Bx + C,$$

where x is the 5-minute average speed for every knot from 1 – 30 kts and A , B , and C are constants. Since there were very few, if any, wind observations above 25 kts for most of the towers, it was unclear whether the stronger wind speeds exhibited the same Weibull characteristics as the lower speeds. However, operational wind speed thresholds exist up to and even beyond 30 kts and the estimation of the peak wind PDFs for these speeds would be useful to the forecasters. As a compromise, the mu and scale parameters were estimated for speeds only to 30 kts.

In order to create modeled probability density functions (PDFs), the shape parameter had to be calculated. It was estimated using the modeled values for scale and mu in the equation

$$\mu = \text{scale} * \Gamma[(\text{shape}+1)/\text{shape}].$$

The gamma function ($\Gamma[\]$) in the equation above is an integral of the form (Wilks 1995)

$$\Gamma(\alpha) = \int_0^{\infty} t^{\alpha-1} e^{-t} dt .$$

A function for this integral exists in S-PLUS and was used to estimate the shape parameter from the modeled mu and scale parameters. The modeled and empirical values of the parameters for Tower 0397 in January are shown in Figure 11. While the modeled trends of all three parameters are smooth up to 30 kts, the empirical trends begin to deviate from the modeled trends at 19 kts, at the location of the large drop-off in the number of observations to below 600. This was a consistent feature seen in other towers and months.

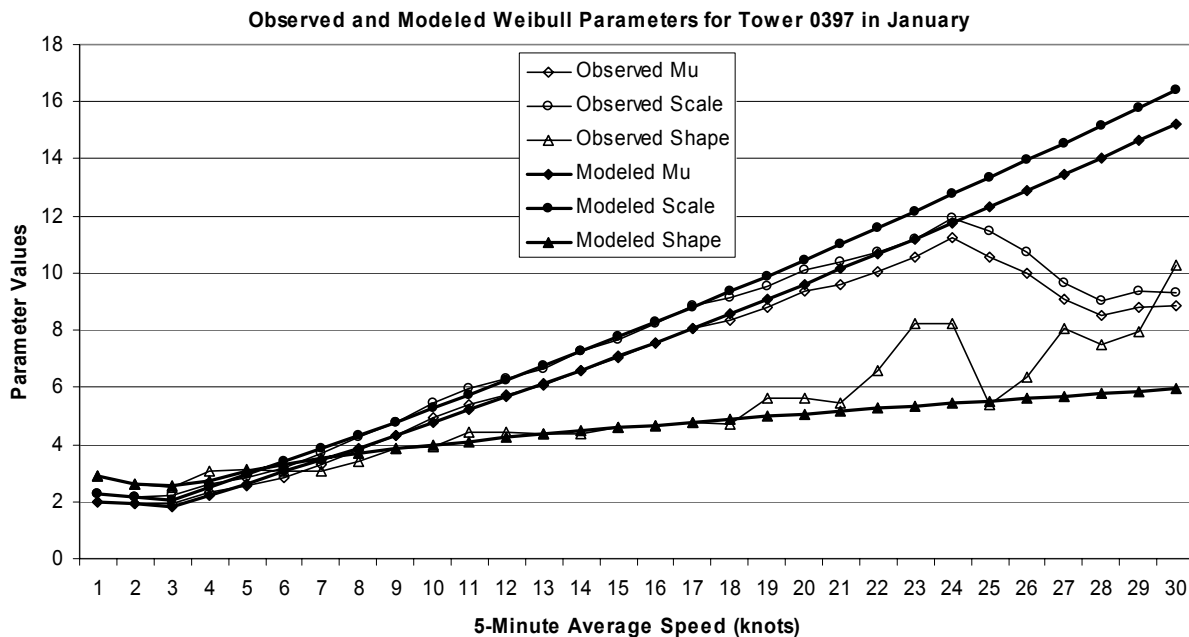


Figure 11. The observed (thin lines) and modeled (thick lines) Weibull scale, mu, and shape parameter values for the peak wind speed PDFs based on the January 5-min average wind speeds from 1 - 30 kts at Tower 0397.

4.4. Analysis of Modeled Distributions

The modeled scale and shape parameters were used to create modeled PDFs for all average wind speeds in the range 1 – 30 kts using the S-PLUS functions. The empirical and modeled PDFs for Tower 0397 at 60 ft in January are shown in Figures 9 (Section 4.1) and 12, respectively. All PDFs in Figure 12 were created using the modeled scale and shape parameters. The trend of the PDFs in Figure 12 is almost identical to that in Figure 9, except for the PDFs at 19 kts and beyond. The modeled PDFs follow a smooth trend of decreasing height and increasing width. Also, the widths and peak PDF values are similar between the empirical PDFs with > 600 observations and the corresponding modeled PDFs indicating that the model is likely valid at these average speeds. The modeled parameters were tested using two methods to check their validity: a standard error test and a gust factor test.

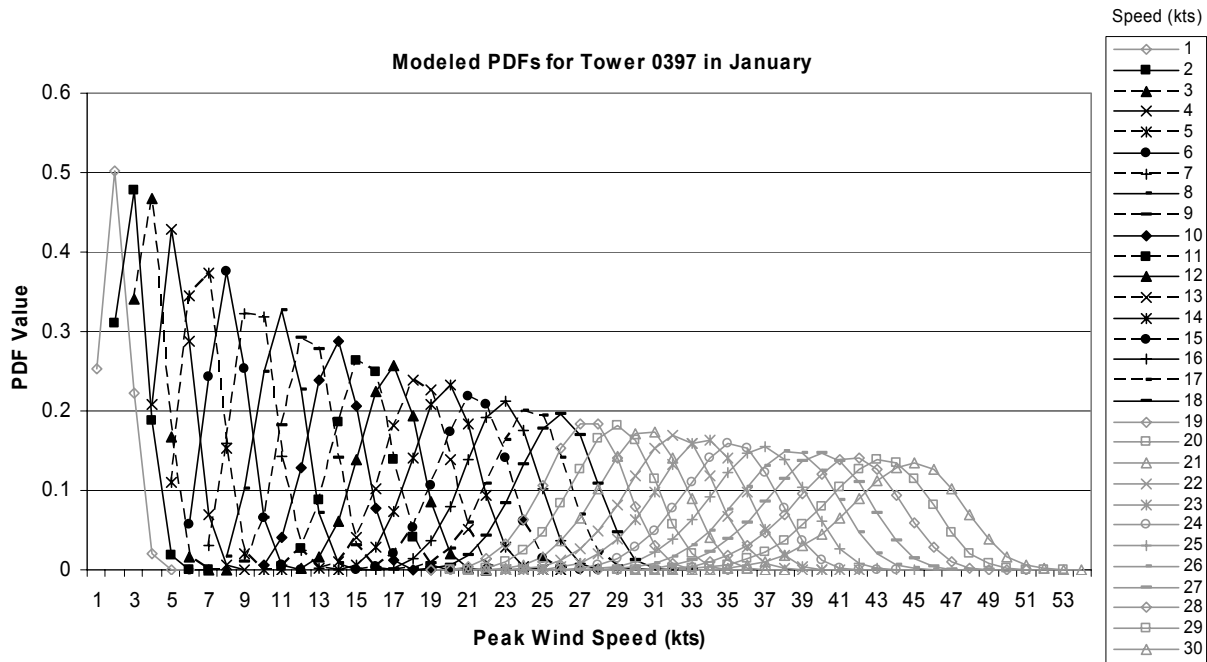


Figure 12. Modeled PDFs of the January peak wind speed distributions associated with each 5-minute average wind speed (see legend) from 1 - 30 kts at Tower 0397/60 ft. The gray lines indicate the PDFs whose parameters were not used to determine polynomial regression equations. The legend shows the 5-minute average speeds associated with each PDF. The black PDFs alternate solid and dashed lines to make them easier to distinguish.

4.4.1. Standard Error Test

Even though the data set was large, it was still considered a sample of the population of KSC/CCAFS wind speed observations. The underlying assumption for the modeled PDFs was that their values represented what the true values would be for the entire population of wind speed observations. A critical test of this assumption is to determine if the modeled parameter values are within 1 or 2 standard errors (SEs) of the empirical parameter values. When the empirical parameters were calculated, S-PLUS also output the SEs. The actual equation for the Weibull SE in S-PLUS is very complex, but can still be described generally by the equation

$$SE = \left(s^2 / n \right)^{1/2},$$

where s is the standard deviation and n is the number of observations. The SE values for the parameters in Figure 10 are shown in Figure 13. The errors are very small where there are a large number of observations, but begin to increase significantly when the number of observations begins to decrease quickly above 18 kts. The SE values for μ and shape are almost identical, but different from the scale SE values, which were much larger. For most towers and months, the μ and shape SEs were similar, but at times they were as large as or even larger than the scale SE. It was always the case that the SE values for all parameters were very small for lower average wind speeds where

the sample sizes were very large, and larger for the higher average wind speeds where the sample size was very small. This result indicates that sample size had a strong effect on the SE value, as seen in the equation above.

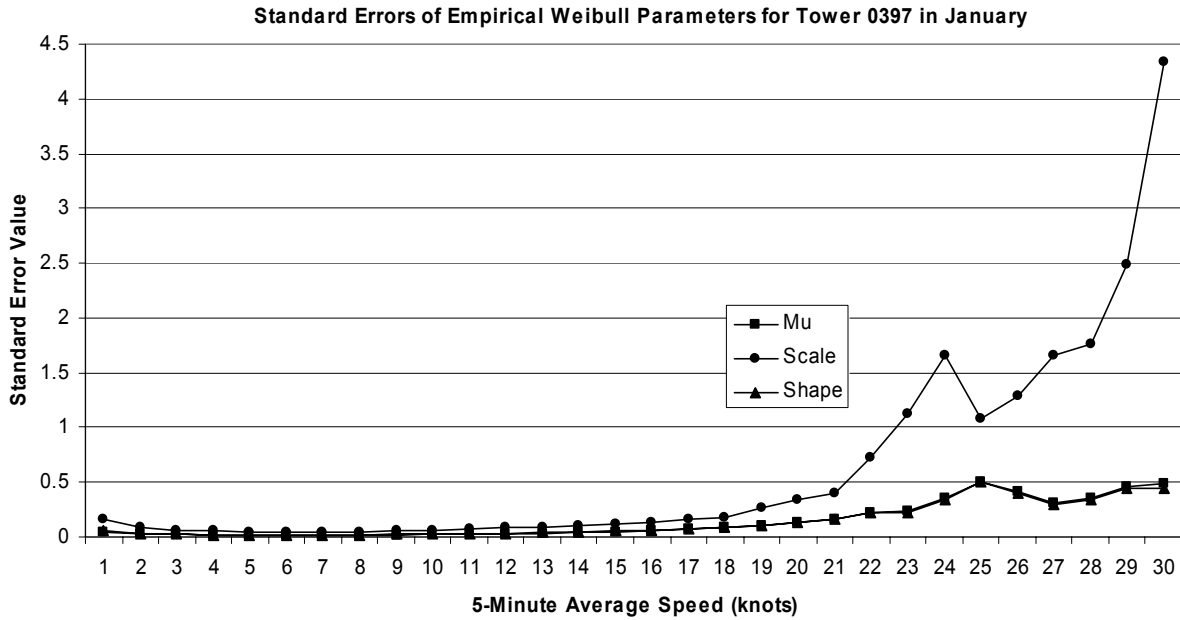


Figure 13. The standard errors of the empirical Weibull mu, scale and shape parameter values in Figure 10.

Once all modeled parameters, empirical parameters, and SEs were calculated, they were used to check whether the modeled parameters were within 2 SEs of the empirical values. First, the absolute value of the difference between each empirical and modeled parameter value at each average speed was calculated:

$$\begin{aligned} \text{MuAbsDif} &= | \text{Mu}_E - \text{Mu}_M |, \\ \text{SclAbsDif} &= | \text{Scl}_E - \text{Scl}_M |, \text{ and} \\ \text{ShpAbsDif} &= | \text{Shp}_E - \text{Shp}_M |, \end{aligned}$$

where the subscript E is represents the empirical parameters and the subscript M represents the modeled parameters.

These difference values were then subtracted from a value that was twice the SE of each parameter:

$$\begin{aligned} \text{MuDif} &= 2 * \text{SE}_{\text{MU}} - \text{MuAbsDif}, \\ \text{SclDif} &= 2 * \text{SE}_{\text{SCL}} - \text{SclAbsDif}, \text{ and} \\ \text{ShpDif} &= 2 * \text{SE}_{\text{SHP}} - \text{ShpAbsDif}. \end{aligned}$$

If the values on the left-hand side of the last three equations were 0 or positive then the modeled parameter values were at or within two SEs of the empirical values. The magnitude would show the extent to which the modeled value was within or outside two SEs of the empirical value.

The values from the last 3 equations are plotted in Figure 14 for each wind speed at Tower 0397 in January. For the average speeds up to approximately 21 kts, the values switch between positive and negative and the magnitudes are very small. The SE values for these speeds are all < 0.5 (Figure 13). It is probably difficult for any modeled value to be within even two SEs of the empirical values since the SE values were so small. Given that the magnitudes of the differences in Figure 14 are so small for average speeds less than 21 kts, it could be assumed that the modeled values are a good approximation of the values for the population. Above 21 kts, the magnitudes of the differences are much larger and most are negative, indicating that the modeled parameter values are well outside two SEs. Charts similar to Figure 14 were created for every tower/height/month combination, and showed somewhat similar results. There were large differences in magnitude between towers and months, but most values were negative. This is an indication that the modeled values at the higher speeds are likely incorrect and should not be used for the development of an operational product.

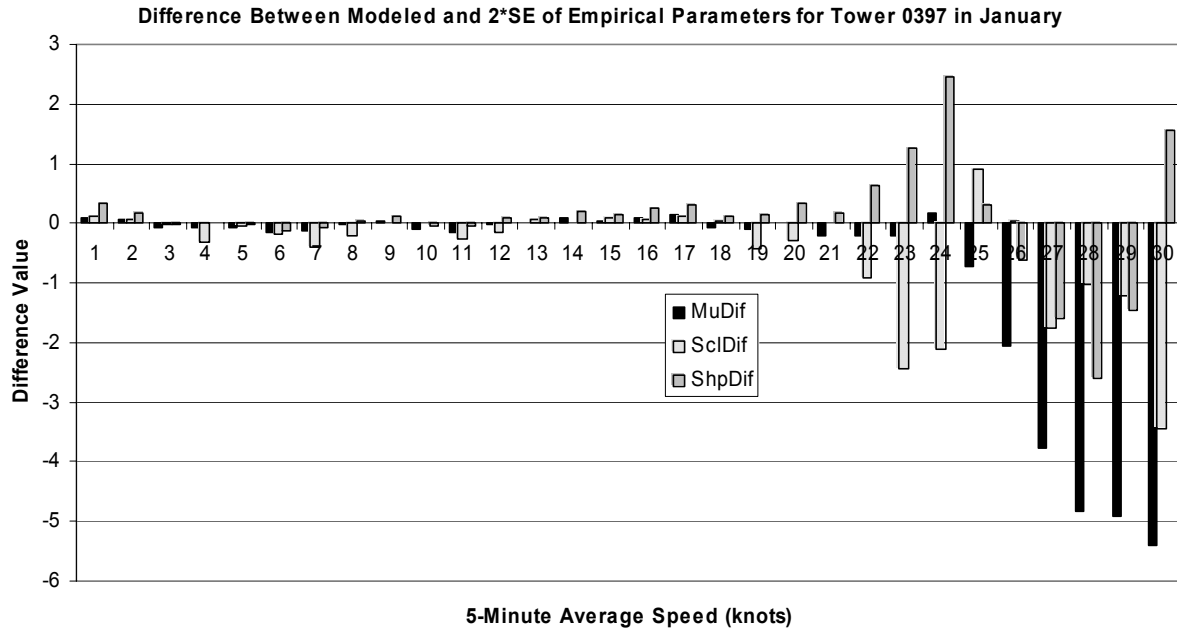


Figure 14. Chart of the differences between two standard errors of the observed parameters and the difference between the empirical and modeled parameter values. The differences are for each parameter at 5-minute average speed for Tower 0397 at 60 ft in January.

4.4.2. Gust Factor Test

The gust factor check was done to determine if the modeled parameters produced gust factors (GFs) consistent with known and accepted empirical values (McVehil and Camnitz 1969, NASA 2000, Hsu 2001). Several formulations exist that estimate the gust factor based on average speed, height above ground, and stability. These formulations are verified using a simple calculation of observed peak speed divided by its associated average wind speed. The values in the literature, both from the formulations and observations, range from 1.2 to 1.6. SMG uses a modified gust factor based on the formulations in McVehil and Camnitz (1969) and NASA (2000). These formulas produce gust factors from 2.5 – 4 at low wind speeds to 1.4 at higher wind speeds. Indeed, McVehil and Camnitz showed that the gust factor decreases with increasing average wind speed. In this test, the modeled and empirical mu parameters were used as the peak speed in the gust factor calculation, given that they were considered the mean peak value in the distribution. Gust factors were calculated using the equation

$$GF = \mu / \text{Average Speed.}$$

The results from the GF calculations for Tower 0397 in January are displayed in Figure 15. All values in the graphs are consistent with those found in the literature. The modeled and empirical GFs are in close agreement from 1 kt up through 20 kts, but begin to diverge somewhat at 21 kts and more markedly beyond 24 kts. The trends for both GFs decrease to a low point for the lower wind speeds, then increase through 24 kts. The empirical trend tends to ‘flatten out’ between 10 and 24 kts and then decreases rapidly to 30 kts. The modeled trend continues a smooth increase for all average speeds above 4 kts. The trends for the other tower/month combinations were similar. The modeled GF usually increased with average speed, sometimes to values above 1.8, while the empirical GF tended to be flat and then decreased for the higher average winds.

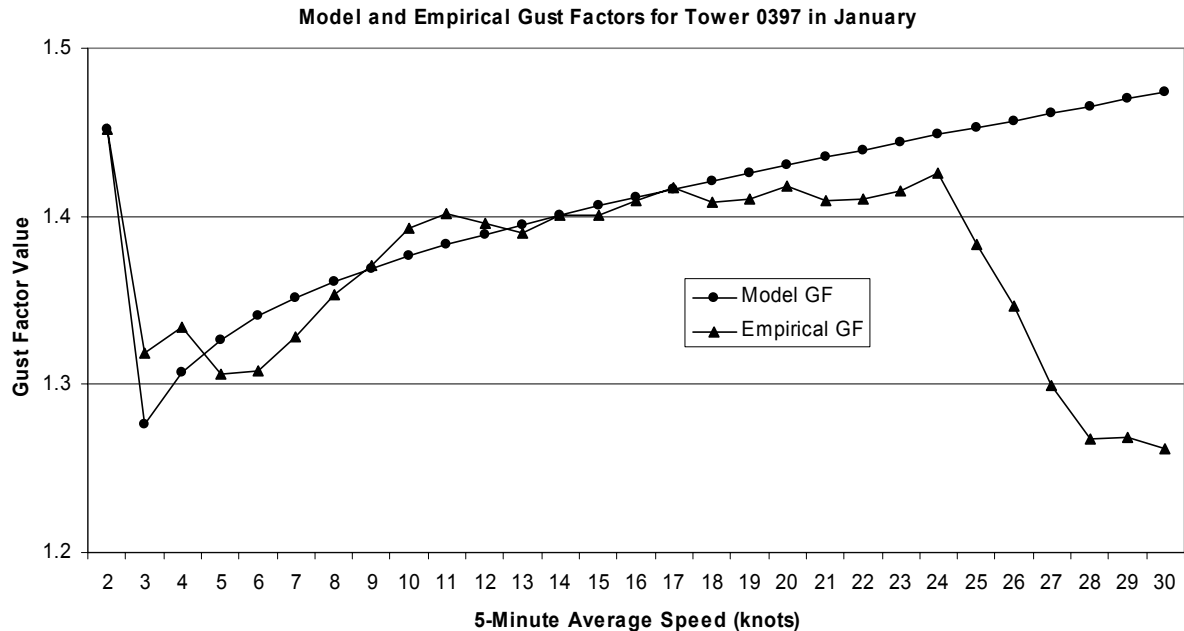


Figure 15. The modeled and empirical gust factors for Tower 0397 at 60 ft in January. The modeled and empirical values for the 1-kt average speed are both 2. It is not shown so that the values for the other average speeds could be discerned more easily.

The results from this test were ambiguous at best. While the modeled GF values were consistent with observed and calculated GF values in the literature, the increasing trend with average wind speed was not. Unfortunately, this test provided no added value in determining the validity of the modeled parameters. Since this test did not provide an obvious result, the conclusion from the SE test will be used: that the modeled PDFs at higher speeds are likely incorrect and should not be used for the development of an operational product.

4.4.3. Interpretation of Results

Because of the scarcity of observations above ~20 kts average speed for most towers, the validity of modeling the peak speed distributions at these speeds was in question. The standard error and gust factor tests were conducted not as absolute tests, but to produce indications of the soundness of the assumptions that all peak speed distributions were Weibull and that their parameters followed a polynomial trend with average speed. The results from neither test supported the assumptions, and the standard error test indicated that modeling the parameters for the higher speeds produced erroneous distributions. It is possible that the Weibull parameters for the peak wind distributions of the higher average speeds do not follow the trend of those for the lower average speeds. It is also possible that the phenomena that create higher average and peak wind speeds produce different theoretical peak wind distributions than Weibull. Regardless of the reason, the distributions for these particular speeds should not be used in operations due to the uncertainty in their accuracy.

On the other hand, the abundance of observations below ~20 kts average speed allowed the assumption that their peak speed distributions were Weibull. The conclusion, therefore, is to provide peak wind Weibull distributions for those average speeds with more than 600 observations in the data set. These PDFs for Tower 0397 at 60 ft in January are shown in Figure 16. The Weibull parameters estimated from the observations (Figure 10) were used to create these distributions with the same S-PLUS function that used the modeled parameters to create the modeled distributions, as in Figure 13. The estimated PDFs in Figure 16 are recommended for operational use over the empirical PDFs since they more likely represent the PDFs of the population of wind speeds.

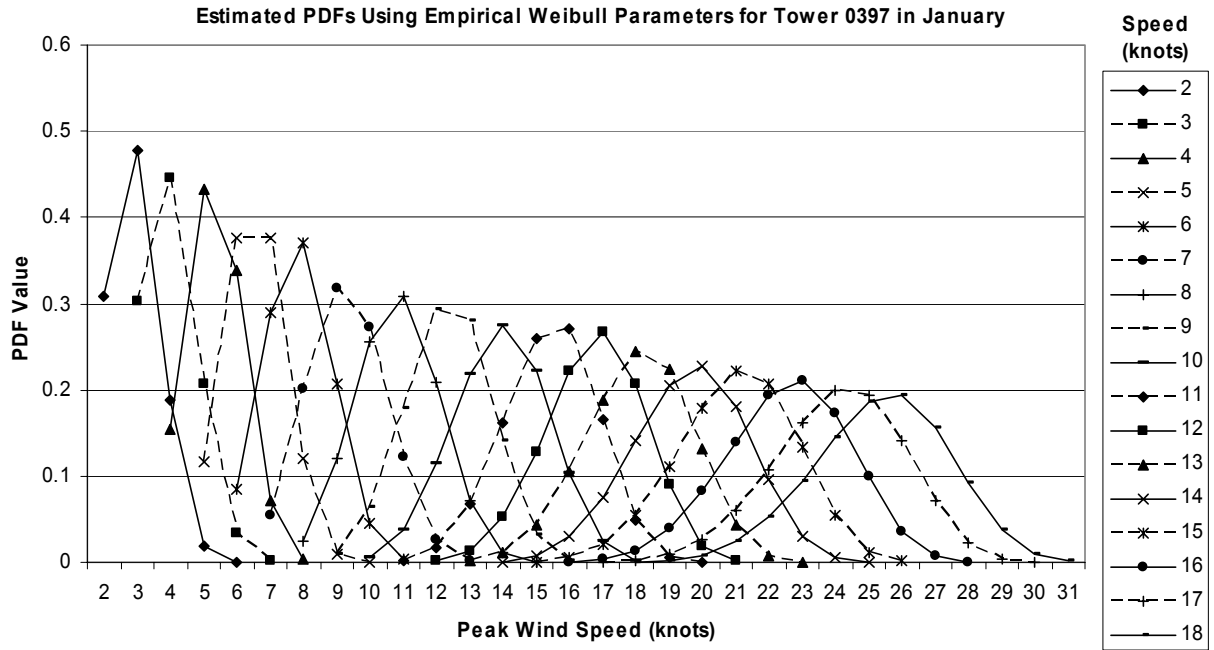


Figure 16. The estimated Weibull PDFs of the January peak wind speed distributions associated with each 5-minute average wind speed (see legend) from 2 - 18 kts for Tower 0397 at 60 ft. The legend shows the 5-minute average speeds associated with each PDF. The PDFs alternate solid (even) and dashed (odd) lines to make them easier to distinguish.

Figure 17 shows the probabilities for the PDFs in Figure 16. A forecaster can identify the curve for a 5-minute average speed of interest, then locate the point on that curve for the 5-minute peak speed of interest and determine the probability of meeting or exceeding that peak speed by the values on the y-axis. For example, if the average wind is observed or forecast to be 12 kts (solid line with solid squares), the probability of meeting or exceeding 15 kts is 0.93, or 93%.

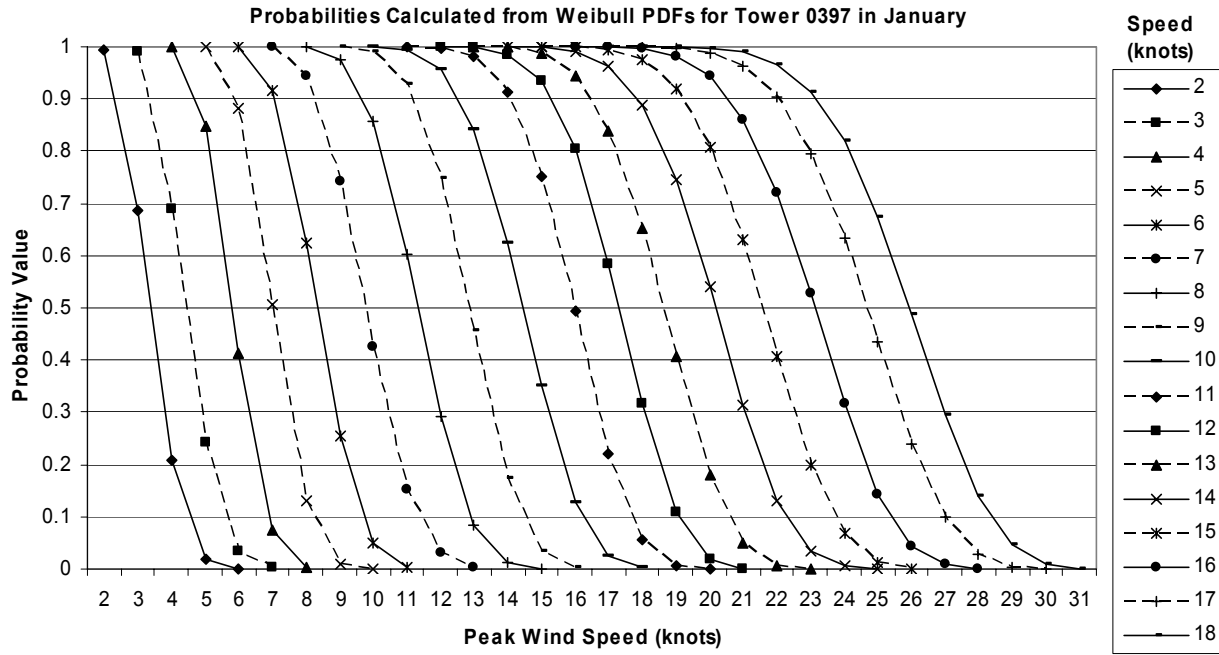


Figure 17. The probability curves for the estimated Weibull PDFs in Figure 16. The curves alternate solid (even) and dashed (odd) lines to make them easier to distinguish.

5. Conclusions

The goal of this task was to develop a peak wind forecasting tool for use in launch, landing, and ground operations at KSC/CCAFS. The 5-minute average and peak wind speed data from the KSC/CCAFS wind tower network were analyzed extensively to develop such a tool. Unfortunately the stratifications, methods, and data used in this study were unable to capture the physical mechanisms that caused gusts so they could be used in a prognostic tool. However, products suitable for use in operations have been developed that allow forecasters to display the climatologies for each tower and to determine the probability of exceeding specific peak speed values at each tower given an observed or forecast average wind speed value.

5.1. Summary and Analysis of Results

The first step in the task was to create climatologies of the average and peak winds to determine their behavior by month, hour and direction, and in relation to each other. Climatologies were created for the three stratifications of month/hour, month/direction, and month/hour/direction. Although the climatologies did show some interesting trends, they were essentially smoothed low frequency values of high frequency and highly variable data. They were unable to help determine the average and peak winds for a particular time on a particular day, and the AMU concluded that the climatological values would be of limited use in the development of forecast equations.

The next step involved creating 5-minute peak wind speed distributions for the 5-minute average wind speeds in 1-kt intervals. The data for each tower/height combination were stratified by month then average wind speed, and the peak speed PDFs for each observed average wind speed was calculated (Figure 9). Tests revealed that the peak speed PDFs for average speeds that were observed 600 times or more in the database resembled the theoretical Weibull distribution. Wind speeds with less than 600 observations were usually greater than ~20 kts, and their PDFs were erratic and not amenable to fitting with an established theoretical distribution.

Still, wind speeds > 20 kts are operationally significant to launch, landing and ground operations. When the Weibull parameters of mu, scale, and shape were plotted against wind speed, it appeared that their trends could be extrapolated to approximate the parameters for these higher average wind speeds (Figure 10). The modeled parameters (Figure 11) and the resulting PDFs (Figure 12) followed smooth trends and appeared realistic. However, the standard error and gust factor tests indicated that the modeled PDFs for the higher wind speeds may not be valid. Rather than allow operational use of a product that the AMU could not prove was reliable, the final decision was to calculate the peak speed PDFs for the average speeds with greater than 600 observations in the data set (Figure 16).

Several factors create higher average wind speeds and influence the intensity of peak winds in the KSC/CCAFS area. The phenomena responsible for high average and peak speeds include synoptic frontal passages, convective outflow boundaries, and the mixing down of high momentum air from aloft. The atmospheric stability in the boundary layer is also a factor for gusts, as is the location of the wind sensor relative to the ocean (i.e. how far inland) and how much vegetation surrounds the site. The peak speed distributions resulting from the effects of any of these factors could have a different set of Weibull parameters or fit a different theoretical distribution altogether. For the average wind speeds with greater than 600 observations, the theoretical Weibull distribution fit the peak speed PDFs very well. It is important to keep in mind, though, that the factors that cause gusts at higher speeds also create gusts at the well-sampled lower speeds. It is possible that the peak speed distributions at these lower average speeds are the sum of a mixture of multiple population samples with different distributions. The different phenomena that cause gusts could be mixed together in the lower speed samples, and each could create their own distribution that is not necessarily Weibull, but the sum of which is approximately Weibull.

The best way to determine the proper distributions would be to create data stratifications based on meteorological phenomena and other physical properties such as stability and topography around the tower. However, stratifying the data by phenomenon would have required time and resources beyond the scope of this task. Hourly surface observations may contain the information necessary to discern times of frontal passages and convection in the area, but a complex algorithm would have to be developed to recognize the patterns and observations associated with differing meteorological phenomena. Even if all information was available to make the appropriate stratifications, it is likely that those stratifications would have produced sample sizes much smaller than 600 observations, too small from which to determine appropriate peak speed distributions.

Three previous AFIT theses (Storch 1999, Cloys 2000, and Coleman 2000) have attempted to produce cool-season peak wind forecasting techniques for operations at KSC/CCAFS without success. They found the development of such a tool to be difficult, and the results from this task underscore that difficulty. The physical mechanisms involved in the creation of wind gusts are complex and are difficult, if not impossible, to discern from the wind observations alone. At the very least, data from other sources such as rawinsondes, surface observations, and profilers should be included in the development of a forecast tool and the data should be stratified by phenomena and other physical properties mentioned earlier. Mesoscale models contain equations that attempt to define the physics responsible for the creation of wind gusts. A combination of several data types with a mesoscale model may be the ideal approach for developing a peak wind forecasting tool.

5.2. Operational Products

Even though a tool to forecast peak winds was not developed, several of the analyses done in this task could be useful to operations. The climatologies described in Section 3 and the PDFs derived from the empirical Weibull parameters described in Section 4 are valid analyses based on the historical behavior of the winds at the towers of interest in Table 1. Forecasters at the 45 WS and SMG have already indicated that one or both of these products would be useful in their analysis and forecasting of winds.

The data for the climatologies were first stratified by tower and height, then month. For the towers with redundant sensors at the same height, separate climatologies were created for each sensor. After this main stratification, there were 3 separate sub-stratifications:

- Hour,
- Direction (10° sectors), and
- Direction (45° sectors) and hour.

The means and standard deviations of the 5-minute average and peak winds were calculated for all three stratifications, and the numbers of observations used in the calculations were summed. Figures 2, 3, and 5 in Section 3 show the means and standard deviations for the hour, direction, and hour and direction stratifications, respectively. The hourly mean values show a noticeable diurnal trend (Figure 1), but the large standard deviations indicate large variability in the winds at every hour. These large values were found for every tower/sensor combination in every month in the analysis. Therefore, the mean values themselves should not be used as absolute forecasts for the average or peak winds.

The average and peak wind means by direction showed no pattern of higher or lower speeds for specific directions, and the standard deviations were as high as those for the hourly stratification (Figure 3). The number of observations in each direction bin showed some interesting features, however (Figure 4). They revealed the most likely wind directions for each month where there was an abundance of observations (NNW in Figure 4) and least likely directions where there was a smaller number of observations.

The average and peak winds in the final stratification of direction and hour revealed more pronounced diurnal trends in both the mean and standard deviation values (Figure 5) than in the hourly stratification. The standard deviations were still high, however. The number of observations in each direction/hour bin focused in on the interesting features of the direction stratification (Figures 6 and 8). Directions which have a large number of observations, e.g. NNW in Figure 4, can be shown by hour to see if there are preferred hours for that particular direction sector, e.g. 1300 – 1800 UTC in Figure 6.

The PDFs in Section 4 can be used to calculate a probability of meeting or exceeding a peak speed value given an observed or forecast 5-minute average wind speed. There were 3 types of PDFs calculated in this task:

- Empirical PDFs calculated directly from the observations,
- Estimated PDFs created from the empirical Weibull parameters, and
- Modeled PDFs created with Weibull parameters estimated from polynomial regression equations.

It is the AMU's recommendation that the modeled PDFs not be transitioned into operations due to the inability to prove their accuracy, as stated earlier. The AMU does recommend that the estimated PDFs and, as in Figures 16 and 17, be used as they are based on sound estimations of the parameters. Since they were calculated directly from the historical observations, the empirical PDFs and probability curves are available if operational personnel choose to use them. The number of observations used to calculate the empirical PDFs are also available.

All of the climatologies, PDFs, and probability curves are currently displayed in MS Excel Pivot Charts. These displays are very flexible, allowing changes to the charts with point-click-drag techniques. Axes can be switched, multiple variables can be represented on one axis, and specific curves can be temporarily removed from the display to facilitate closer examination of other curves. This is the product that is available as a result of the current AMU tasking and training will be provided on how to use the Pivot Charts.

5.3. Future Work

5.3.1. Predicting Gusts with a Numerical Weather Prediction Model

A method to estimate wind gusts using the physical processes estimated by model data rather than empirical data was proposed by Brasseur (2001). The basic assumption in that study was that wind gusts result from the deflection of air parcels from higher in the boundary layer which are brought down to the surface by turbulent eddies. The wind gust was estimated as the maximum wind speed of boundary layer parcels for which the turbulent energy was greater than the buoyant energy between the surface and the height of the parcels. The study also developed upper and lower bound calculations around the wind gust estimate that should have a high probability of containing the observed gusts. These calculations were based on physical processes in the boundary layer. The results showed that the bounding interval was reliable for both daily and hourly gust estimations, but was highly dependent on the accuracy of the model. The gust estimate tended to be 3-10% less than the observed gusts. Burk and Thompson (2002) found the method appealing because of its use of physical processes, rather than statistical methods, to estimate wind gusts. They modified the Brasseur algorithms to include the effects of clouds in the boundary layer, and are using output from the Coupled Ocean-Atmosphere Mesoscale Prediction System to test both algorithms. No results have been reported to date.

The models used in the Brasseur study were run at 25 km and 50 km resolution. The Eta and Regional Atmospheric Modeling System (RAMS) model output are available over KSC/CCAFS at 12 km and 1.25 km resolutions, respectively. The higher resolution of these models would capture more localized effects which may produce more accurate wind gust forecasts. The forecasts, however, would be highly dependent on the accuracy of the model output. Nonetheless, these models contain the physical processes and equations necessary for the estimation and forecasting of wind gusts, and future tasks should consider the possibility of testing the Brasseur method for an operational peak wind forecasting tool.

Another approach considered is that of using a Kalman filter (Kalman 1960) with single-station wind tower data to make short-term forecasts of the peak winds. Such a forecast would require the use of a reliable, reasonably accurate underlying model, such as the previously discussed RAMS or Eta. McGinley (2001) had success using a Kalman filter to develop and QC a temperature database. The Kalman filter in that study was meant to provide updated estimates of temperature by combining temperature observations with modeled values. Specifically, it was composed of the trend from a station time series, trend information from surrounding stations, and trends from the Rapid Update Cycle (RUC) model, or the Eta if the RUC was not available. However, as with the Brasseur study, the results may be highly dependent on the accuracy of the underlying model.

5.3.2. Shuttle Landing Facility Towers

In a follow-on task, the AMU will create the PDFs of the 10-minute peak winds given the 5-minute peak wind at the Shuttle Landing Facility (SLF) towers (0511 – 0513) for SMG. Since SMG uses 10-minute peak winds, the 10-minute peak wind for each 5-minute average wind will be determined by comparing the 5-minute peak associated with the current 5-minute average and the 5-minute peak from the previous 5-minute period. The maximum of the two will be considered the 10-minute peak. The first step will be to determine which theoretical distribution best describes the observed PDFs. The Weibull distribution best described the 5-minute peak PDFs in the current task, but it is possible that a distribution other than Weibull would best fit the 10-minute peak PDFs.

Once the appropriate theoretical distribution is determined and the resulting PDFs calculated, the AMU will develop a PC-based graphical user interface (GUI) or dialog box that will allow customers quick access to the information they need. The AMU anticipates using the features in MS Excel to build this tool. The simplest scenario is for the customer to enter an average and a peak wind speed value, then the GUI would return the probability of the peak wind to equal or exceed the input peak value based on the input average value. Another possibility would be to input an average value and output the probabilities for every peak wind value associated with that average value, either in tabular or graphical form. The customer will be consulted at almost every step in the development of this GUI to ensure the end product is what the customer needs, wants and will use.

References

- Brasseur, O., 2001: Development and application of a physical approach to estimating wind gusts. *Mon. Wea. Rev.*, **129**, 5-25.
- Burk, S. D., and W. T. Thompson, 2002: Comments on "Development and application of a physical approach to estimating wind gusts." *Mon. Wea. Rev.*, **130**, 1933-1935.
- Cloys, K. P., 2000: A neural network solution to predicting wind speed at Cape Canaveral's Atlas Launch Pad. M.S. Thesis, AFIT/GM/ENP/00M-03, Department of Engineering Physics, Air Force Institute of Technology, 132 pp. [Available from Air Force Institute of Technology, Wright-Patterson Air Force Base, OH 45433].
- Coleman, L. K., 2000: Use of climatology to predict maximum wind speeds at the Kennedy Space Center and Cape Canaveral Air Station. M.S. Thesis, AFIT/GM/ENP/00M-04, Department of Engineering Physics, Air Force Institute of Technology, 61 pp. [Available from Air Force Institute of Technology, Wright-Patterson Air Force Base, OH 45433].
- Hsu, S. A., 2001: Spatial variations in gust factor across the coastal zone during Hurricane Opal in 1995. *Nat. Wea. Digest.*, **25**, No. 1,2, 21-23.
- Insightful Corporation, 2000: *S-PLUS@6 User's Guide*, Insightful Corp., Seattle, WA, 470 pp.
- Jagger, T., J. B. Elsner, X. Niu, 2001: A dynamic probability model of hurricane winds in coastal counties of the United States. *J. Appl. Meteor.*, **40**, 853-863.
- Justus, C. G., W. R. Hargraves, A. Mikhail, and D. Graber, 1978: Methods for estimating wind speed frequency distributions. *J. Appl. Meteor.*, **17**, 350-353.
- Kalman, R., 1960: A new approach to linear filtering and prediction problems. *Trans. ASME, Ser. D, J, Basic Eng.*, **82**, 35-45.
- McGinley, J. A., 2001: Toward a surface data continuum: Use of the Kalman filter to create a continuous quality controlled surface data set. *14th Conference on Numerical Weather Prediction*, Ft. Lauderdale, FL. Amer. Met. Soc., 127-131.
- McVehil, G. E. and H. G. Camnitz, 1969: Ground Wind Characteristics at Kennedy Space Center. NASA Contractor Report CR-1418, Kennedy Space Center, FL, 102 pp.
- National Aeronautics and Space Administration, 2000: Terrestrial Environment (Climatic) Criteria Handbook for use in Aerospace Vehicle Development. NASA-HDBK-1001, Section 2, 142 pp. [Available online at <http://standards.nasa.gov>].
- Pavia, E. G. and J. J. O'Brien, 1986: Weibull statistics of wind speed over the ocean. *J. Climate Appl. Meteor.*, **25**, 1324-1332.
- Storch, S. J., 1999: Predicting launch pad winds at the Kennedy Space Center with a neural network model. M.S. Thesis, AFIT/GM/ENP/99M-06, Department of Engineering Physics, Air Force Institute of Technology, 60 pp. [Available from Air Force Institute of Technology, Wright-Patterson Air Force Base, OH 45433].
- Tuller, S. E. and A. C. Brett, 1984: The characteristics of wind velocity that favor the fitting of a Weibull distribution in wind speed analysis. *J. Climate Appl. Meteor.*, **23**, 124-134.
- Van der Auwera, L., F. de Meyer, and L. M. Malet, 1980: The use of the Weibull three-parameter model for estimating mean wind power densities. *J. Appl. Meteor.*, **19**, 819-825.
- Wilks, D. S., 1995: *Statistical Methods in the Atmospheric Sciences*. Academic Press, Inc., San Diego, CA, 467 pp.

List of Acronyms

45 WS	45th Weather Squadron
AFIT	Air Force Institute of Technology
AMU	Applied Meteorology Unit
CCAFS	Cape Canaveral Air Force Station
ELV	Expendable Launch Vehicle
EST	Eastern Standard Time
FR	Flight Rules
GF	Gust Factor
KSC	Kennedy Space Center
LCC	Launch Commit Criteria
MARSS	Meteorological And Range Safety Support
PDF	Probability Density Function
RAMS	Regional Atmospheric Modeling System
RUC	Rapid Update Cycle
QC	Quality Control
SE	Standard Error
SLC	Space Launch Complex
SMG	Spaceflight Meteorology Group
UTC	Universal Coordinated Time

NOTICE

Mention of a copyrighted, trademarked or proprietary product, service, or document does not constitute endorsement thereof by the author, ENSCO, Inc., the AMU, the National Aeronautics and Space Administration, or the United States Government. Any such mention is solely to inform the reader of the resources used to conduct the work reported herein.